


 Cite this: *RSC Adv.*, 2025, 15, 46925

# A review of metal ion complexation/decomplexation reaction-based fluorescent sensors for detecting biological thiols

 Nguyen Khoa Hien,<sup>a</sup> Mai Van Bay,<sup>b</sup> Quan V. Vo,<sup>c</sup> Son Tung Ngo,<sup>de</sup>  
 Doan Thanh Nhan,<sup>f</sup> Pham Cam Nam<sup>g</sup> and Duong Tuan Quang<sup>\*h</sup>

Biothiols such as glutathione (GSH), cysteine (Cys), and homocysteine (Hcy) are essential to many physiological and biochemical processes in humans, and their abnormal levels are associated with various health disorders. Fluorescent sensors based on metal ion complexation/decomplexation have emerged as powerful tools for the selective and sensitive detection of these thiols. This review highlights recent advances in biothiol sensing systems mediated by metal ions. Complexes of Cu<sup>2+</sup> and Hg<sup>2+</sup> have been most extensively investigated, while only limited studies involve ions such as Fe<sup>3+</sup> and Ag<sup>+</sup>. The discussion emphasizes sensor mechanisms elucidated through analyses of reaction pathways, coordination chemistry, redox properties, stability constants, together with investigations of biothiol speciation at different pH values and their reactions with metal ions. Additional considerations include detection limits, selectivity, reusability, and applications. Although the structural similarity of GSH, Cys, and Hcy makes their discrimination challenging, several sensors exploit steric or redox differences to achieve selectivity. These insights clarify current challenges and highlight future directions for rational sensor design.

Received 28th September 2025

Accepted 2nd November 2025

DOI: 10.1039/d5ra07368e

[rsc.li/rsc-advances](http://rsc.li/rsc-advances)

## 1 Introduction

Cysteine (Cys), glutathione (GSH), and homocysteine (Hcy) are non-protein biological thiols that play crucial roles in various physiological and biochemical functions in humans.<sup>1–3</sup>

Cys is a precursor for protein synthesis and plays a vital role in protecting cells from damage caused by free radicals and oxidative agents. Additionally, Cys is involved in detoxification processes by binding to heavy metals and other toxic substances, aiding in their removal from the body.<sup>4</sup> The intracellular concentration of Cys ranges from 30 to 200 μM.<sup>5</sup> The highest concentration of Cys in plasma has been found to reach up to 250 μM.<sup>1</sup> Changes in Cys levels have been shown to be associated with

several diseases such as Alzheimer's and Parkinson's disease, autoimmune deficiency syndrome, and hyperhomocysteinemia.<sup>1</sup>

Glutathione is a tripeptide composed of three amino acids: L-glutamate, L-cysteine, and L-glycine. It is the most abundant non-protein thiol in cells, with intracellular concentrations ranging from 1 to 15 mM, primarily in its reduced form.<sup>6</sup> GSH is one of the body's most powerful antioxidants, protecting cells from oxidative damage by neutralizing free radicals.<sup>6,7</sup> It plays a critical role in detoxification, particularly in the liver, where it helps eliminate harmful substances and convert them into less toxic forms.<sup>8</sup> Additionally, GSH is essential for maintaining and regulating the immune system.<sup>6</sup> It is also believed to be associated with diseases, including cancer, stroke, heart disease, pancreatic and kidney disorders, diabetes, Alzheimer's, Parkinson's, gastritis, peptic ulcers, and atherosclerosis.<sup>6,7</sup>

Homocysteine (Hcy) is formed in the body from the metabolism of methionine. Hcy acts as an intermediate in the one-carbon metabolism cycle, participating in methylation processes, the regeneration of methionine, and the synthesis of cysteine. The balance of Hcy in the body is maintained through pathways that either regenerate methionine or convert it into cysteine.<sup>9</sup> Hcy levels in the blood typically range from 5 to 13 μM.<sup>10</sup> Elevated levels of Hcy in the blood, known as hyperhomocysteinemia, are associated with several serious health conditions, particularly cardiovascular, neurological, and bone-related diseases. Hyperhomocysteinemia can also affect fertility in both men and women, leading to recurrent miscarriages or infertility.<sup>11–14</sup>

<sup>a</sup>Mien Trung Institute for Scientific Research, Vietnam National Museum of Nature, Vietnam Academy of Science and Technology, Hue 49000, Vietnam

<sup>b</sup>The University of Danang, University of Science and Education, Danang 50000, Vietnam

<sup>c</sup>Faculty of Chemical Technology-Environment, The University of Danang - University of Technology and Education, 48 Cao Thang, Danang 50000, Vietnam

<sup>d</sup>Laboratory of Biophysics, Institute for Advanced Study in Technology, Ton Duc Thang University, Ho Chi Minh City 72915, Vietnam

<sup>e</sup>Faculty of Pharmacy, Ton Duc Thang University, Ho Chi Minh City 72915, Vietnam

<sup>f</sup>Quang Ngai Department of Education and Training, Quang Ngai 53000, Vietnam

<sup>g</sup>The University of Danang – University of Science and Technology, Danang 50000, Vietnam. E-mail: pcnam@dut.udn.vn

<sup>h</sup>Department of Chemistry, Hue University, Hue 49000, Vietnam. E-mail: dtquang@hueuni.edu.vn



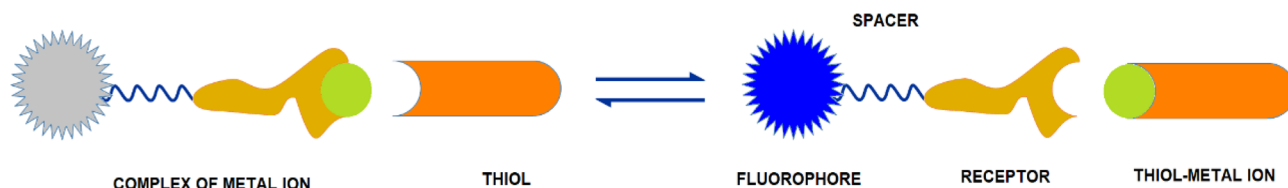


Fig. 1 The operating mechanism of the metal complexes as fluorescent sensors for detecting thiols based on the metal ion complexation/decomplexation reactions.

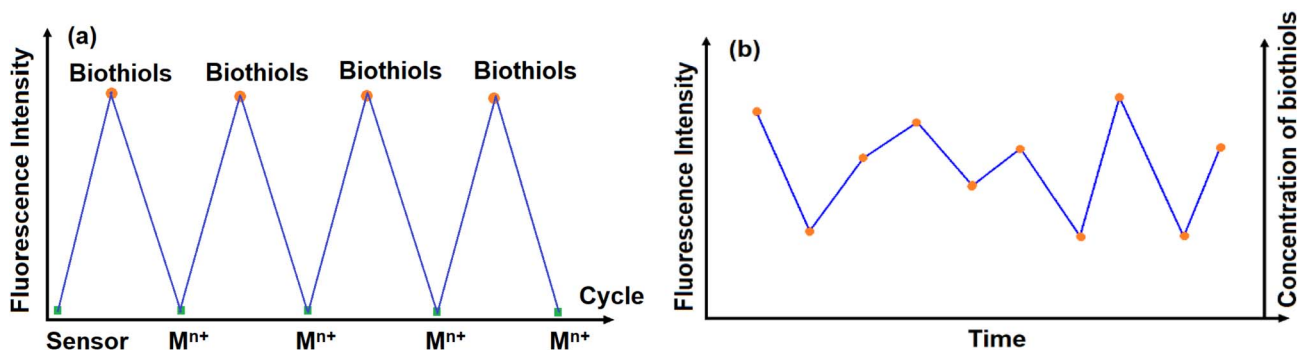


Fig. 2 (a) The change in fluorescence intensity of the metal complex sensor solution upon the alternate addition of biothiols and metal ions, respectively; (b) the change in fluorescence intensity of the metal complex sensor solution over time and at different biothiol concentrations.

Given the important roles of Cys, GSH, and Hcy, various methods for their determination have been developed, including high-performance liquid chromatography,<sup>1,15</sup> gas chromatography-mass spectrometry,<sup>16</sup> electrochemistry,<sup>17</sup> and UV-vis absorption and fluorescence spectroscopy.<sup>18–20</sup> Among these, fluorescent sensors have garnered significant interest from scientists due to their high sensitivity, simple analysis methods, and ability to monitor in living cells.<sup>21–25</sup>

To date, numerous fluorescent sensors for detecting biothiols have been reported based on various mechanisms, including ring formation with aldehyde,<sup>26–28</sup> nucleophilic addition reactions (e.g., Michael addition),<sup>29,30</sup> protein/peptide ligation reactions (Native Chemical Ligation, NCL),<sup>31</sup> aromatic substitution–rearrangement reactions,<sup>32,33</sup> cleavage of sulfonamide or sulfonate esters by thiols,<sup>34,35</sup> disulfide cleavage by thiols,<sup>36,37</sup> dual-recognition molecular probes,<sup>38</sup> and metal ion complexation/decomplexation reactions.<sup>39,40</sup> Among these, fluorescent sensors based on metal ion complexation/decomplexation reactions (Fig. 1) have garnered particular interest from scientists due to their superior characteristics. The reusability of these sensors was reported in several studies, based on monitoring the changes in fluorescence intensity of the sensor solution during the alternate addition of biothiols and metal ions (Fig. 2a). In this process, the metal complex-based sensors initially exhibited either quenched or enhanced fluorescence, depending on their coordination state. Upon the addition of biothiols, these molecules competed with the ligands for metal binding, releasing the ligands and thereby restoring or altering the fluorescence signal. Subsequent re-addition of the metal ions reversed this process, demonstrating that the sensors could be reused multiple times.<sup>20,40</sup> Moreover, the reversible interactions of these sensors with biothiols indicated their potential for developing sensors

capable of monitoring biothiol concentration changes in real time. Fig. 2b illustrated the variation in fluorescence intensity of the sensors with biothiol concentration and over time. Such sensors were considered highly valuable for continuously monitoring biothiol levels in biological samples. This quantitative capability was essential for clinical diagnostics, where tracking biothiol concentrations could provide insights into various diseases, such as oxidative stress or cancer progression. Unfortunately, no sensors with such functionality have been reported to date. Despite these advantages, the sensors also have certain limitations, especially in the selective detection of individual biothiols, due to the structural similarities and comparable complexation abilities of biothiols with metal ions.<sup>20,39,40</sup>

This review focuses on evaluating recent research on fluorescent sensors for biothiol detection based on metal ion complexes. This review is not intended to be exhaustive but rather to highlight current research findings through an analysis of sensitivity, selectivity, advantages, and limitations in applications, based on notable sensors recently reported in the literature.

## 2 Structure of GSH, Cys, and Hcy, and their pH-dependent forms

The biothiols GSH, Cys, and Hcy share similar structures, consisting of an amino acid skeleton, a sulfur atom in the sulfhydryl group, and a hydrogen atom in the sulfhydryl group (Fig. 3). These biothiols differ in their amino acid skeleton, leading to variations in the chemical activity of the S and H atoms in the sulfhydryl group.<sup>41</sup>

One of the key differences that can be highlighted is the acid dissociation constants ( $pK_a$ ) of biothiols, as these are



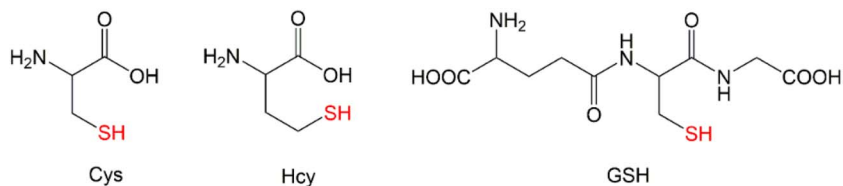
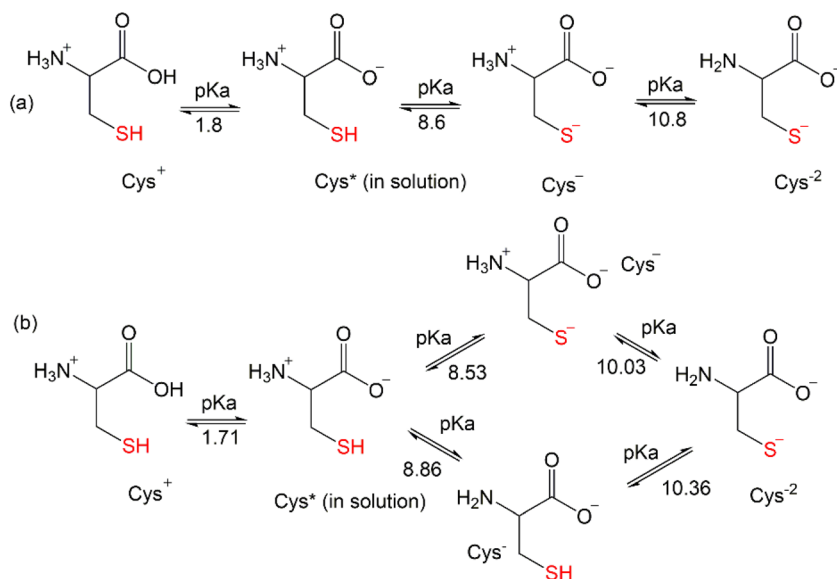
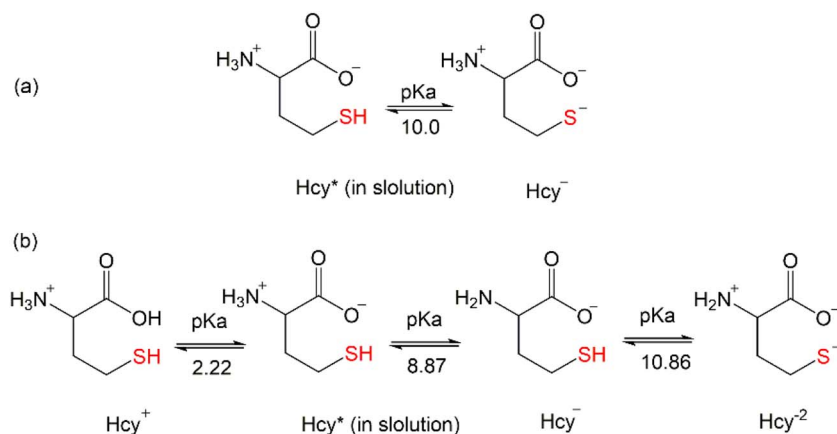


Fig. 3 The structures of biothiols.

Fig. 4 The  $pK_a$  values and existing forms of Cys,<sup>42,43</sup> redrawn based on data reported in ref. 42 and 43.

related to their existing forms in solution, which result in variations in their chemical activities, particularly their ability to form complexes with metal ions. Specifically, Cys exists in four forms depending on the pH, with the neutral pH form being Cys\* (Fig. 4).<sup>42,43</sup> Hcy exists in four forms depending on the pH, with the neutral pH form being Hcy\* (Fig. 5).<sup>44,45</sup> GSH exists in five forms depending on the pH, with the neutral pH form being GSH<sup>-</sup> (Fig. 6).<sup>46–49</sup>

Notably, an important distinguishing characteristic among Cys, Hcy, and GSH is the acid dissociation constant ( $pK_a$ ) of the –SH group, which directly participates in complex formation with some metal ions. Their  $pK_a$  values are 8.6, 10.8, and 9.6, respectively.<sup>42–49</sup> This difference is believed to be the reason for the selective recognition of Cys, Hcy, and GSH by certain sensors.<sup>50</sup> To gain a better understanding of the existing forms of Cys, Hcy, and GSH in solution, the molar

Fig. 5 The  $pK_a$  values and existing forms of Hcy,<sup>44,45</sup> redrawn based on data reported in ref. 44 and 45.

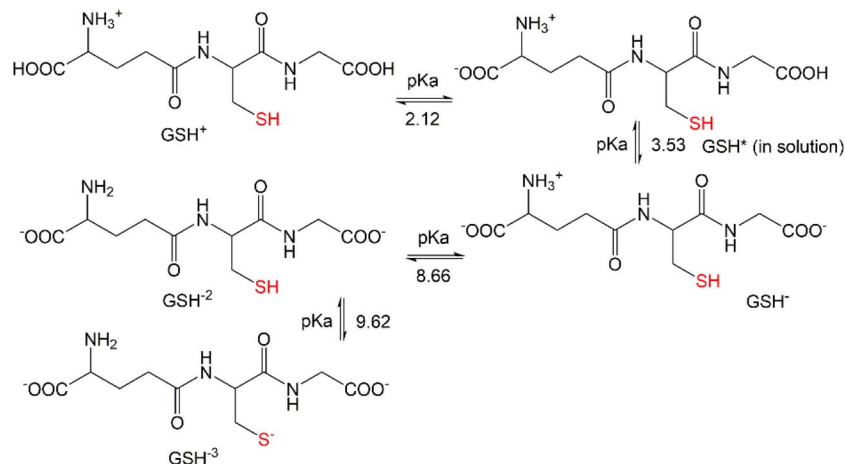


Fig. 6 The  $pK_a$  values and existing forms of GSH,<sup>46–49</sup> redrawn based on data reported in ref. 46–49.

fraction values of the species at different pH levels were calculated and presented in Tables 1–3. These results were obtained from the equations used to calculate the molar fractions of species in polyprotic acid solutions  $H_nA$  (eqn (1)–(3)):<sup>51</sup>

$$\alpha_{H_nA} = \frac{[H^+]^n}{D} \quad (1)$$

$$\alpha_{H_{n-1}A} = \frac{K_1[H^+]^{n-1}}{D} \quad (2)$$

$$\alpha_{H_{n-j}A} = \frac{K_1K_2\dots K_j[H^+]^{n-j}}{D} \quad (3)$$

where:

$$D = [H^+]^n + K_1[H^+]^{n-1} + K_1K_2[H^+]^{n-2} + \dots + K_1K_2\dots K_n \quad (4)$$

$K_1, K_2, K_3, \dots, K_n$  were the dissociation constants of the first, second, third, ...,  $n$ th acidic protons.

The calculation results in Tables 1–3 show that, for Cys, the  $S^-$  containing species predominate in solution at pH around 9–10. In contrast, for Hcy, the  $S^-$  containing species

Table 2 Mole fraction of the species of Hcy present in solution as a function of pH

pH	$H_3L^+$	$H_2L$	$HL^-$	$L^{2-}$	Sum
1	0.943168	0.056832	0.000000	0.000000	1.000000
2	0.624002	0.375998	0.000000	0.000000	1.000000
3	0.142337	0.857662	0.000001	0.000000	1.000000
4	0.016325	0.983662	0.000013	0.000000	1.000000
5	0.001657	0.998209	0.000135	0.000000	1.000000
6	0.000166	0.998487	0.001347	0.000000	1.000000
7	0.000016	0.986672	0.013310	0.000002	1.000000
8	0.000001	0.880992	0.118843	0.000164	1.000000
9	0.000000	0.422372	0.569763	0.007865	1.000000
10	0.000000	0.061156	0.824967	0.113877	1.000000
11	0.000000	0.003105	0.418796	<b>0.578099</b>	1.000000
12	0.000000	0.000050	0.067547	<b>0.932403</b>	1.000000
13	0.000000	0.000001	0.007192	<b>0.992807</b>	1.000000
14	0.000000	0.000000	0.000724	<b>0.999276</b>	1.000000

Table 1 Mole fraction of the species of Cys present in solution as a function of pH

pH	$H_3L^+$	$H_2L$	$HL^-$	$L^{2-}$	Sum
1	0.863193	0.136807	0.000000	0.000000	1.000000
2	0.386863	0.613137	0.000000	0.000000	1.000000
3	0.059351	0.940647	0.000002	0.000000	1.000000
4	0.006270	0.993705	0.000025	0.000000	1.000000
5	0.000630	0.999119	0.000251	0.000000	1.000000
6	0.000063	0.997432	0.002505	0.000000	1.000000
7	0.000006	0.975487	0.024503	0.000004	1.000000
8	0.000001	0.798985	0.200696	0.000318	1.000000
9	0.000000	0.281556	<b>0.707236</b>	0.011209	1.000000
10	0.000000	0.033223	<b>0.834516</b>	0.132262	1.000000
11	0.000000	0.001538	0.386268	0.612194	1.000000
12	0.000000	0.000024	0.059350	0.940627	1.000000
13	0.000000	0.000000	0.006270	0.993730	1.000000
14	0.000000	0.000000	0.000631	0.999369	1.000000

Table 3 Mole fraction of the species of GSH present in solution as a function of pH

pH	$H_4L^+$	$H_3L$	$H_2L^-$	$HL^{2-}$	$L^{3-}$	Sum
1	0.929298	0.070494	0.000208	0.000000	0.000000	1.000000
2	0.561493	0.425936	0.012570	0.000000	0.000000	1.000000
3	0.092383	0.700797	0.206820	0.000000	0.000000	1.000000
4	0.003325	0.252241	0.744417	0.000016	0.000000	1.000000
5	0.000043	0.032766	0.966980	0.000212	0.000000	1.000000
6	0.000000	0.003370	0.994454	0.002176	0.000001	1.000000
7	0.000000	0.000331	0.978216	0.021401	0.000051	1.000000
8	0.000000	0.000028	0.816955	0.178730	0.004287	1.000000
9	0.000000	0.000001	0.269355	0.589285	0.141360	1.000000
10	0.000000	0.000000	0.013270	0.290314	<b>0.696416</b>	1.000000
11	0.000000	0.000000	0.000183	0.040011	<b>0.959806</b>	1.000000
12	0.000000	0.000000	0.000002	0.004151	<b>0.995847</b>	1.000000
13	0.000000	0.000000	0.000000	0.000417	<b>0.999583</b>	1.000000
14	0.000000	0.000000	0.000000	0.000042	<b>0.999958</b>	1.000000



predominate in solution at pH 11–14, whereas for GSH, the  $S^-$  containing species predominate in solution at pH 10–14.

### 3 The complexation/decomplexation reaction-based sensors for biothiols

#### 3.1 Sensors based on the complexation/decomplexation of $Cu^{2+}$ ions

**3.1.1 Sensors based on  $Cu^{2+}$  complexes.** To date, sensors for biothiol detection based on the complexation/decomplexation of  $Cu^{2+}$  ions have been developed more frequently than those based on other metal ions. Juyoung Yoon and co-authors reported a  $Cu^{2+}$  ion complex with the fluorescent compound  $F_1$ , serving as a fluorescent sensor ( $F_1-Cu^{2+}$ ) for biothiol detection *via* metal ion complexation/decomplexation reactions (Fig. 7a). In HEPES/DMSO solution (95/5, v/v, 10 mM, pH 7.4),  $F_1$  displayed strong fluorescence at a maximum wavelength of 450 nm, with an excitation wavelength of 355 nm.  $F_1$  formed a 1 : 1 molar complex with

$Cu^{2+}$ , which resulted in fluorescence quenching. Upon the addition of GSH, Cys, or Hcy, the fluorescence of  $F_1-Cu^{2+}$  was restored, corresponding to the release of free  $F_1$  through the decomplexation of  $F_1-Cu^{2+}$  and the simultaneous formation of a thiol- $Cu^{2+}$  complex. This approach allowed the quantitative detection of GSH in the 0–8  $\mu M$  concentration range (using 1  $\mu M$   $F_1-Cu^{2+}$ ), with a detection limit of 0.16  $\mu M$ , even in the presence of various amino acids and proteins such as Ala, Arg, Gln, Glu, Gly, Lys, Met, Phe, Ser, Tyr, Thr, Val, Leu, Ile, Pro, Trp, Asp, Asn, HSA, insulin, lactoferrin, and lysozyme. The method was successfully applied to detect endogenous GSH in cells and living tissues, offering advantages such as low toxicity, minimal background fluorescence, and the capability for deep-tissue imaging (Fig. 7b). However, it could not discriminate between GSH, Cys, and Hcy.<sup>39</sup>

Zhiqiang Zhang and colleagues developed a fluorescent sensor for detecting biothiols based on the  $F_2-Cu^{2+}$  complex, formed from the fluorescent compound  $F_2$  with  $Cu^{2+}$  in a 1 : 1 molar ratio. The  $F_2-Cu^{2+}$  complex reacted with biothiols,

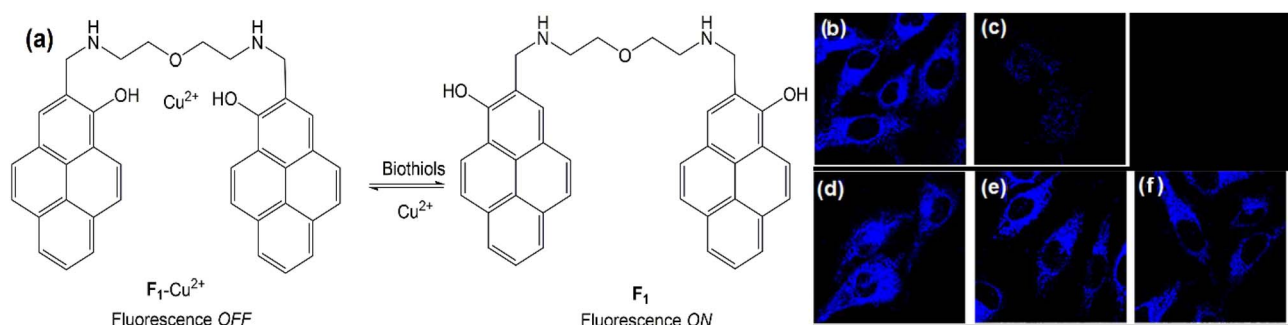


Fig. 7 (a) The sensing mechanism of  $F_1-Cu^{2+}$  for biothiols; (b)–(f) Fluorescence images of  $F_1-Cu^{2+}$  in the live cells: (b) HeLa cells were incubated with  $F_1-Cu^{2+}$ , (c) and incubated with *N*-methylmaleimide (a thiol reactive reagent), (d) and incubated with GSH, (e) Cys, (f) Hcy,<sup>39</sup> adapted with permission from ref. 39, Y. Hu, C. H. Heo, G. Kim, E. J. Jun, J. Yin, H. M. Kim and J. Yoon, *Anal. Chem.*, 2015, **87**, 3308–3313. Copyright 2015 American Chemical Society.

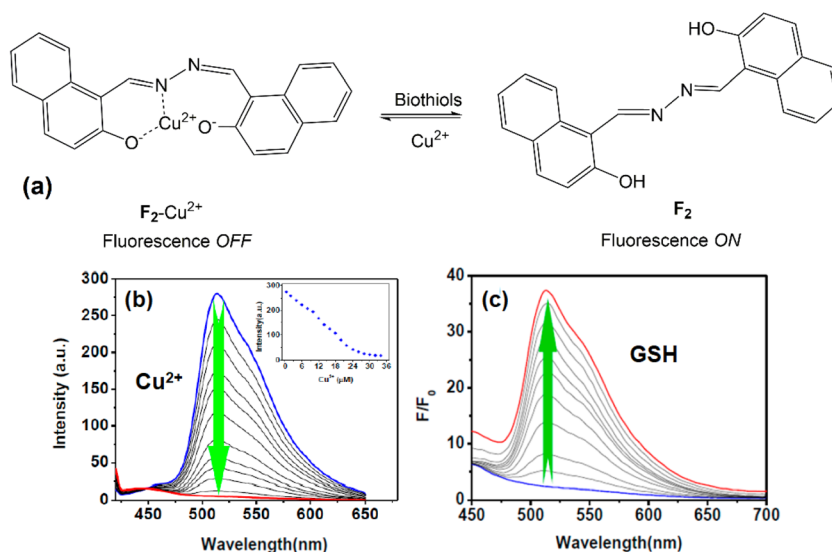


Fig. 8 (a) Complex exchange reaction between  $F_2-Cu^{2+}$  and biothiols, and (b) and (c) fluorescence signal change,<sup>40</sup> adapted from ref. 40, H. Jia, M. Yang, Q. Meng, G. He, Y. Wang, Z. Hu, R. Zhang and Z. Zhang, *Sensors*, 2016, **16**, 79, copyright 2016, MDPI. Licensed under a Creative Commons Attribution 4.0 International Licence.



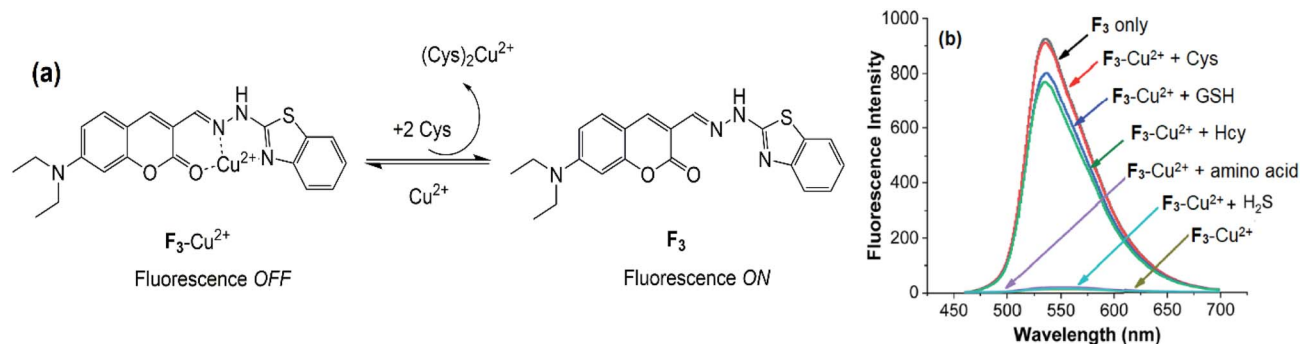


Fig. 9 (a) Reaction between  $F_3\text{-Cu}^{2+}$  and Cys, and (b) fluorescence signal changes of  $F_3\text{-Cu}^{2+}$  upon reaction with GSH, Cys, Hcy, various amino acids, and  $\text{H}_2\text{S}$ ,<sup>19</sup> adapted from ref. 19, N. K. Hien, M. Van Bay, P. D. Tran, N. T. Khanh, N. D. Luyen, Q. V. Vo, D. U. Van, P. C. Nam & D. T. Quang, *RSC Adv.*, 2020, **10**, 36265–36274, copyright 2020, The Royal Society of Chemistry. Licensed under a Creative Commons Attribution 3.0 Unported Licence.

including Hcy, Cys, and GSH, through a complex-exchange mechanism, releasing free  $F_2$  and leading to an almost complete recovery of both fluorescence and UV-vis spectra nm in DMF/HEPES buffer (3 : 7, v/v, pH 7.4) (Fig. 8).  $F_2\text{-Cu}^{2+}$  functioned as an OFF/ON-type fluorescent sensor, selectively detecting biothiols in the presence of other amino acids, including Leu, Ala, Arg, Asn, Asp, Gln, Glu, Gly, His, Lys, Met, Phe, Pro, Ser, Thr, Trp, and Val. The detection limits for Hcy, Cys, and GSH were determined to be 1.5  $\mu\text{M}$ , 1.0  $\mu\text{M}$ , and 0.8  $\mu\text{M}$ , respectively, indicating that  $F_2\text{-Cu}^{2+}$  was sufficiently sensitive for identifying biothiols in biological systems. Moreover, when biothiols and  $\text{Cu}^{2+}$  were alternately added to the  $F_2\text{-Cu}^{2+}$  solution, the fluorescence intensity exhibited reversible “ON–OFF–ON” switching over more than five cycles, demonstrating that the sensor could be reused at least five times. The potential of  $F_2\text{-Cu}^{2+}$  for biothiol detection in A549 human lung cancer cells was further confirmed through fluorescence microscopy imaging.<sup>40</sup>

Nguyen Khoa Hien and co-authors developed an  $F_3\text{-Cu}^{2+}$  complex as a fluorescent sensor for biothiol detection. The formation of the  $F_3\text{-Cu}^{2+}$  complex through the reaction between  $\text{Cu}^{2+}$  and the coumarin derivative  $F_3$  in a 1 : 1 molar ratio resulted in fluorescence quenching of  $F_3$  at 536 nm. Biothiols, particularly Cys, GSH, and Hcy, reacted with  $F_3\text{-Cu}^{2+}$ , releasing free  $F_3$  and restoring its fluorescence intensity. The  $F_3\text{-Cu}^{2+}$

complex exhibited selective sensitivity toward biothiols in the order of  $\text{Cys} > \text{GSH} > \text{Hcy}$ , even in the presence of other amino acids, including Ala, Asp, Arg, Gly, Glu, Ile, Leu, Lys, Met, Thr, Ser, Tyr, Trp, Val, and His (Fig. 9). The reaction occurred in an ethanol/HEPES buffer (1 : 1, v/v, pH 7.4). At a concentration of 5  $\mu\text{M}$ ,  $F_3\text{-Cu}^{2+}$  enabled the detection of Cys with a detection limit of 0.3  $\mu\text{M}$  and a linear range from 0.3 to 10  $\mu\text{M}$ .<sup>19</sup>

A complex  $F_4\text{-Cu}^{2+}$ , formed between the fluorescent compound  $F_4$  and  $\text{Cu}^{2+}$  in a 1 : 1 molar ratio, was reported to function as a fluorescent sensor for Hcy and Cys detection in a  $\text{CH}_3\text{CN}/\text{HEPES}$  buffer (1 : 1, v/v, pH 7.4). The  $F_4\text{-Cu}^{2+}$  sensor reacted with both Cys and Hcy, releasing the free  $F_4$  molecule and thus operating as a fluorescence OFF–ON sensor (Fig. 10). At a concentration of 5  $\mu\text{M}$ ,  $F_4\text{-Cu}^{2+}$  enabled the detection of Cys and Hcy with detection limits of 0.17  $\mu\text{M}$  and 0.25  $\mu\text{M}$ , and linear ranges of 2–8  $\mu\text{M}$  and 2–13  $\mu\text{M}$ , respectively. Amino acids such as Thr, Asp, Leu, Ile, Pro, Met, Glu, Trp, Gly, Ser, Asn, Phe, Gln, Tyr, Arg, Lys, His, Ala, and Val did not interfere with the determination of Cys and Hcy, while the effect of GSH was not investigated in this study. Moreover, the concentrations of Cys and Hcy required to fully restore the fluorescence intensity of the 5  $\mu\text{M}$   $F_4\text{-Cu}^{2+}$  solution were not reported.<sup>52</sup>

A complex between the fluorescent compound  $F_5$  and  $\text{Cu}^{2+}$  in a 1 : 1 molar ratio,  $F_5\text{-Cu}^{2+}$ , was reported as a fluorescent sensor

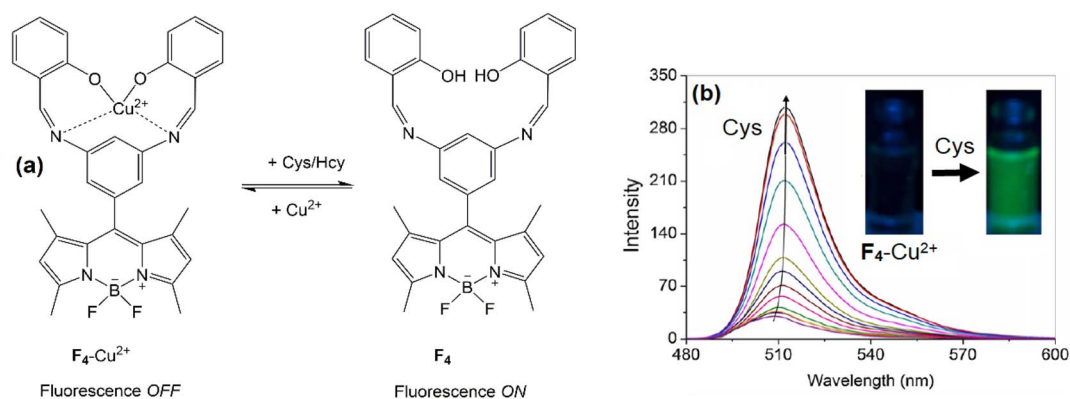


Fig. 10 (a) Reaction of the  $F_4\text{-Cu}^{2+}$  sensor with Cys/Hcy, and (b) their fluorescence changes,<sup>52</sup> adapted from ref. 52, Q. Li, Y. Guo and S. Shao, *Sens. Actuators B Chem.*, 2012, **171**, 872–877. Copyright 2012, with permission from Elsevier.



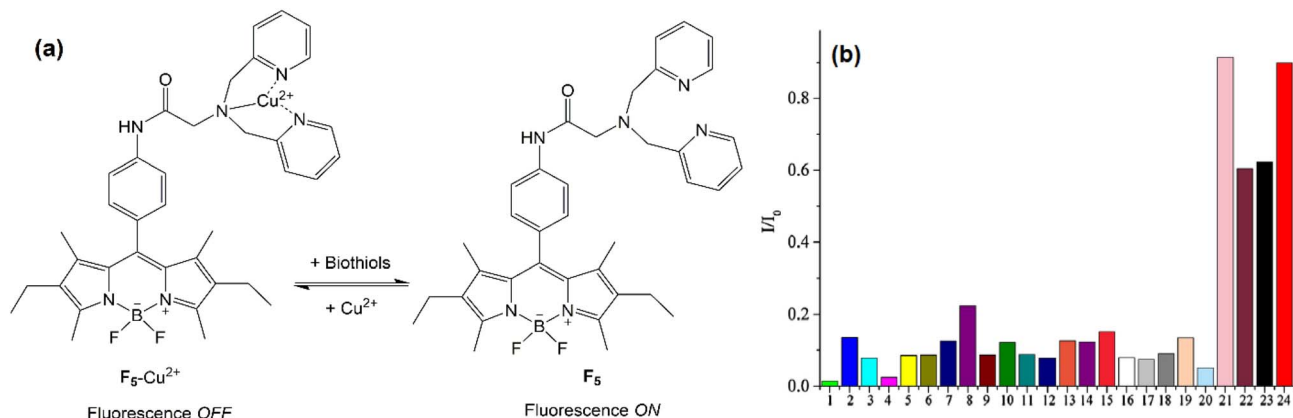


Fig. 11 (a) Sensing mechanism of  $F_5\text{-Cu}^{2+}$  for biothiols, and (b) fluorescence changes of (1)  $F_5\text{-Cu}^{2+}$  upon the addition of (2–20) other amino acids, (21)  $\text{Na}_2\text{S}$ , (22) Cys, (23) Hcy, and (24) GSH,<sup>53</sup> adapted from ref. 53, C.-C. Zhao, Y. Chen, H.-Y. Zhang, B.-J. Zhou, X.-J. Lv and W.-F. Fu, *J. Photochem. Photobiol. A Chem.*, 2014, **282**, 41–46. Copyright 2014, with permission from Elsevier.

for detecting biothiols in the presence of various amino acids (including Ala, Arg, Asn, Asp, Gln, Glu, Gly, His, Ile, Leu, Lys, Phe, Pro, Ser, Thr, Trp, Tyr, and Val), operating *via* a complexation/decomplexation mechanism in an OFF–ON fluorescence mode (Fig. 11). The sensor  $F_5\text{-Cu}^{2+}$  was reported to detect GSH more effectively than Cys and Hcy due to a stronger fluorescence recovery. The sensor  $F_5\text{-Cu}^{2+}$  ( $5\ \mu\text{M}$ ) was able to detect GSH within a linear range of  $0\text{--}30\ \mu\text{M}$ . At a GSH concentration of  $30\ \mu\text{M}$ , the fluorescence intensity of the  $F_5\text{-Cu}^{2+}$  ( $5\ \mu\text{M}$ ) solution is almost fully restored to that of the free  $F_5$  ( $5\ \mu\text{M}$ ) solution. Hence, further increasing the GSH concentration does not alter the fluorescence intensity of the solution.<sup>53</sup>

A complex between the fluorophore  $F_6$  and  $\text{Cu}^{2+}$  was identified with a 1 : 1 molar coordination ratio based on Job's plot titration and ESI-MS spectra. The formation of the  $F_6\text{-Cu}^{2+}$

complex triggers the PET process from the receptor group to the fluorophore in  $F_6$ , leading to a non-fluorescent  $F_6\text{-Cu}^{2+}$  complex (Fig. 12). Biothiols react with the  $F_6\text{-Cu}^{2+}$  complex to release free  $F_6$ , thereby restoring fluorescence. The fluorescence recovery efficiency increases in the order of Hcy, Cys, and GSH, with respective values of 31%, 35%, and 82%. Consequently,  $F_6\text{-Cu}^{2+}$  can serve as a fluorescent sensor for detecting GSH in the presence of various amino acids in a  $\text{CH}_3\text{OH}/\text{HEPES}$  buffer system (9 : 1, v/v, pH = 7.2), with a detection limit of  $0.20\ \mu\text{M}$ . The reusability of this sensor was examined through alternate additions of  $\text{Cu}^{2+}$  and GSH over four cycles (Fig. 12b). This approach was tested on HeLa cells and demonstrated effective detection of GSH under biological conditions.<sup>54</sup>

Another sensor for biothiols, based on a complex of  $\text{Cu}^{2+}$  ions with a coumarin derivative ( $F_7$ ) at a 1 : 2 molar ratio, was

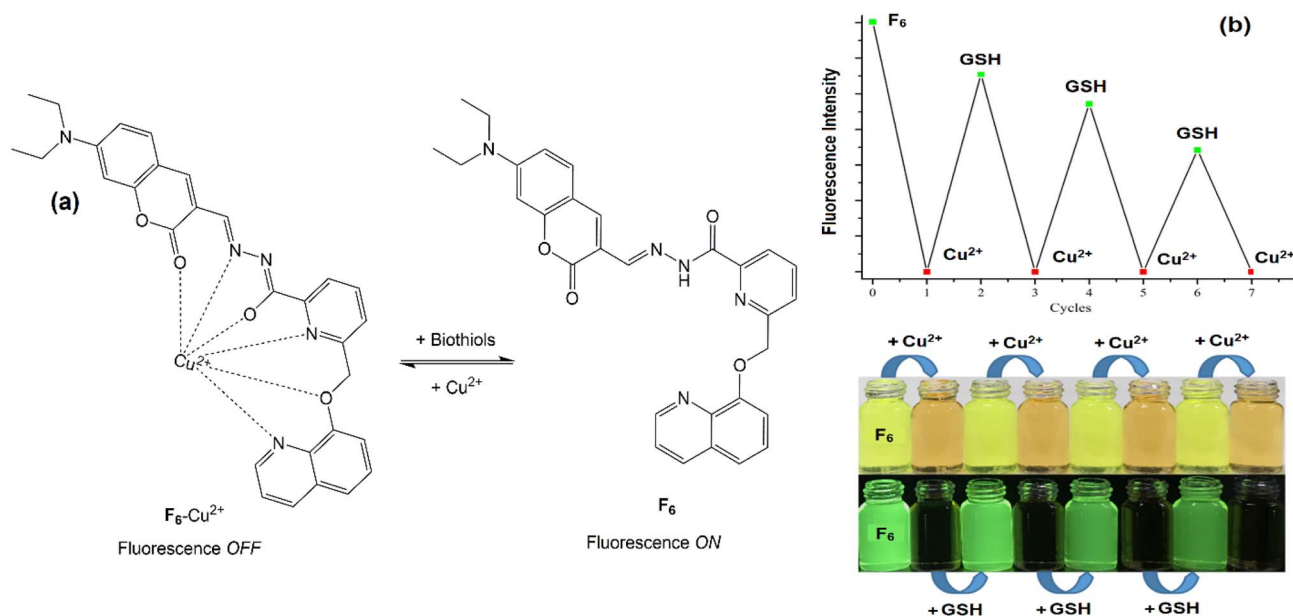


Fig. 12 (a)  $F_6\text{-Cu}^{2+}$  sensor for biothiols, and (b) changes in color (top) and fluorescence (bottom) upon successive additions of  $\text{Cu}^{2+}$  and GSH over four cycles,<sup>54</sup> adapted from ref. 54, S. Li, D. Cao, X. Meng, Z. Hu, Z. Li, C. Yuan, T. Zhou, X. Han and W. Ma, *Bioorg. Chem.*, 2020, **100**, 103923. Copyright 2020, with permission from Elsevier.



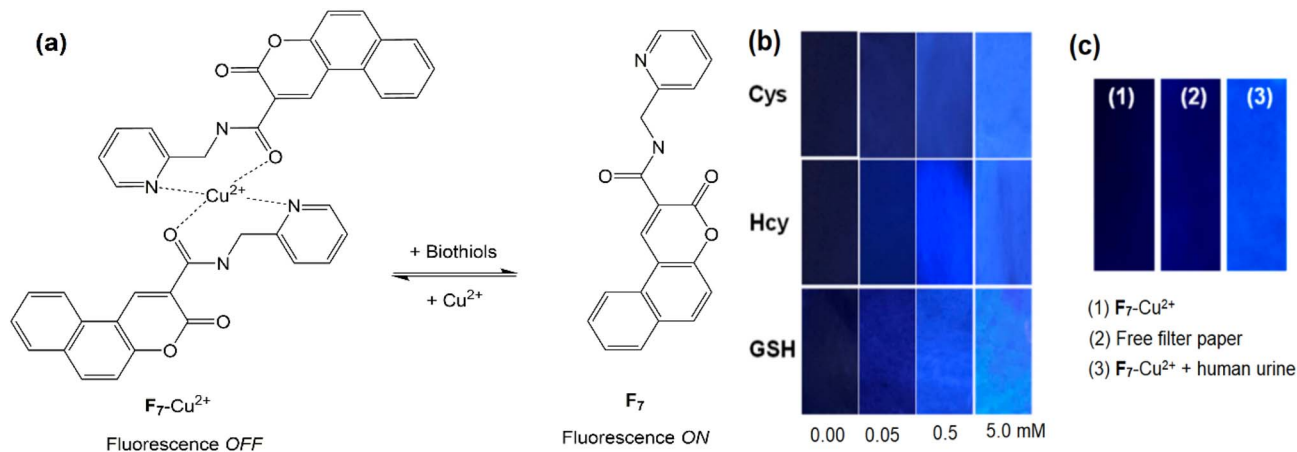


Fig. 13 (a) Biothiol sensor based on the  $(F_7)_2-Cu^{2+}$  complex, (b)  $(F_7)_2-Cu^{2+}$ -impregnated filter paper for biothiol detection, and (c)  $(F_7)_2-Cu^{2+}$ -impregnated filter paper for detecting biothiols in human urine,<sup>55</sup> adapted from ref. 55, Y. Wang, H. Feng, H. Li, X. Yang, H. Jia, W. Kang, Q. Meng, Z. Zhang & R. Zhang, *Sensors*, 2020, 20, 1331, copyright 2020, MDPI. Licensed under a Creative Commons Attribution 4.0 International Licence.

reported (Fig. 13). The  $(F_7)_2-Cu^{2+}$  complex detected biothiols through a decomplexation mechanism operating in an OFF-ON fluorescence mode. This mechanism was confirmed by UV-vis and fluorescence titration spectra of the  $(F_7)_2-Cu^{2+}$  solution with biothiols, as the final spectra were similar to those of the free  $F_7$  under the same conditions. GSH, Hcy, and Cys reacted with the  $(F_7)_2-Cu^{2+}$  complex, enhancing the fluorescence intensity by 5.9-, 5.5-, and 5.3- fold, respectively, compared with the initial intensity. Meanwhile, several other amino acids did not cause any significant change in the fluorescence signal of the  $(F_7)_2-Cu^{2+}$  solution. The molar ratios of GSH, Hcy, and Cys to the  $(F_7)_2-Cu^{2+}$  complex required to achieve maximum fluorescence intensity were approximately 35:1, 40:1, and 70:1, respectively. The  $(F_7)_2-Cu^{2+}$  sensor was capable of detecting GSH, Hcy, and Cys with detection limits of 0.44, 0.68, and 0.96  $\mu$ M, respectively. Similar to other sensors operating *via* the complexation/decomplexation mechanism, the  $(F_7)_2-Cu^{2+}$  sensor was reusable for detecting biothiols for at least five cycles. Notably, the  $(F_7)_2-Cu^{2+}$  sensor exhibited a wide working pH range from 5 to 11, implying that it could not distinguish individual biothiols (GSH, Hcy, and Cys) based on pH changes. This sensor was coated onto filter paper strips and successfully

applied for the visual detection of biothiols in human urine under 365 nm UV light (Fig. 13b).<sup>55</sup>

Tianyun Wang and co-authors reported two fluorescent sensors for the detecting Cys and GSH based on complexes formed between  $Cu^{2+}$  ions and anthracene-derived fluorescent compounds (Fig. 14). These complexes, identified as  $(F_8)_3-(Cu^{2+})_2$ , were nearly non-fluorescent. Cys and GSH reacted with these complexes, releasing free  $F_8$  and restoring fluorescence intensity, while other amino acids caused no significant change in the fluorescence signal. Based on available literature, the authors proposed that the reaction between the two  $(F_8)_3-(Cu^{2+})_2$  complexes and Cys/GSH involved both substitution and redox processes. In this mechanism,  $Cu^{2+}$  ions reacted with Cys and GSH to form  $Cu^{2+}(Cys)_2$  and  $Cu^{2+}(GSH)_2$  intermediates, which subsequently converted into  $Cu^+-CSSC$  and  $Cu^+-GSSG$  products.<sup>56</sup>

Daoben Zhu and colleagues reported a complex of  $Cu^{2+}$  with the fluorescent compound  $F_9$  in a 2:1 molar ratio, which served as a fluorescent sensor for detecting Cys, Hcy, and GSH through an OFF-ON fluorescence mechanism at micromolar concentrations in 0.1 M NaCl and 0.05 M HEPES solution (pH 7) (Fig. 15).<sup>57</sup>

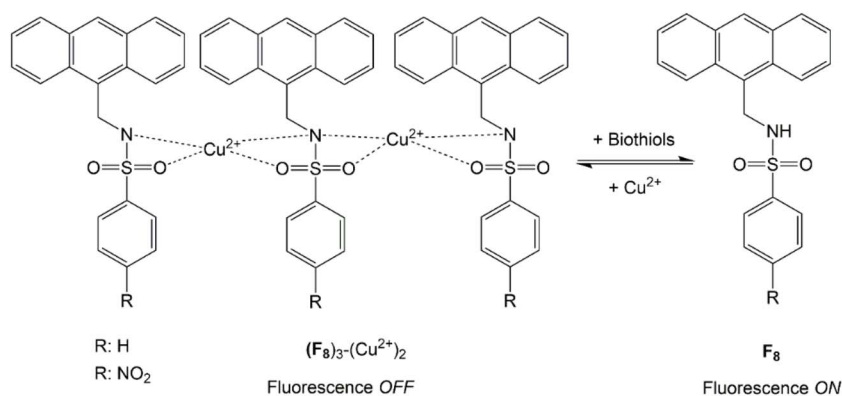


Fig. 14 Fluorescent sensor for biothiol detection based on the complex between  $Cu^{2+}$  and an anthracene derivative,  $(F_8)_3-(Cu^{2+})_2$ ,<sup>56</sup> redrawn based on data reported in ref. 56, C. Li, X. Shang, Y. Chen, H. Chen and T. Wang, *J. Mol. Struct.*, 2019, 1179, 623–629, copyright 2019.



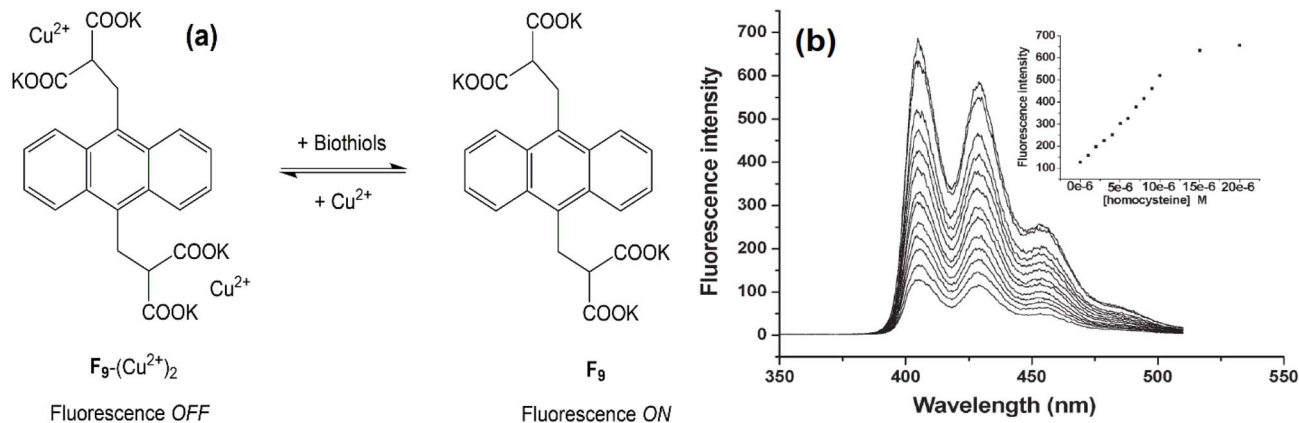


Fig. 15 (a)  $F_9-(Cu^{2+})_2$  complex sensor for biothiols, and (b) fluorescence titration spectra of the  $F_9-(Cu^{2+})_2$  solution with Hcy,<sup>57</sup> adapted from ref. 57 with permission from the Royal Society of Chemistry, Y. Fu, H. Li, W. Hu and D. Zhu, *Chem. Commun.*, 2005, 3189–3191, copyright 2005.

Xiao-Feng Yang and colleagues reported a fluorescent sensor operating *via* an ON–OFF mechanism based on a  $Cu^{2+}$  complex with a rhodamine derivative ( $F_{10}$ ) in an ethanol/water (4/6, v/v) solution containing Tris–HCl buffer at pH 7.1 (Fig. 16). The sensor detected Cys with a detection limit of 0.14  $\mu M$ . Amino acids lacking thiol groups did not interfere with the detection, while the effects of GSH and Hcy were not examined.<sup>58</sup>

Jong Seung Kim and his research group reported another sensor for biothiols based on a complex formed between an iminocoumarin derivative ( $F_{11}$ ) and  $Cu^{2+}$  ions in a 1 : 1 molar ratio. The  $F_{11}-Cu^{2+}$  complex acted as a fluorescent OFF–ON sensor for the selective detection of biothiols in the presence of various amino acids lacking thiol groups. Unlike the previously described sensors, this system did not operate reversibly upon alternating additions of  $Cu^{2+}$  ions and biothiols. NMR spectral analysis of the reaction product between  $F_{11}$  and  $Cu^{2+}$  revealed the hydrolysis of the iminocoumarin compound, yielding a new aldehyde derivative ( $F_{11-s}$ ) and leading to a change in fluorescence signal (Fig. 17a). The detection limit for GSH in aqueous solution using the  $F_{11}-Cu^{2+}$  sensor was  $10^{-8}$  M, and similar behavior was observed for the  $Cu^+$  complex. The sensor was further applied for biothiol detection in HepG2 cells using confocal fluorescence microscopy. HepG2 cells not pretreated with NEM (*N*-ethylmaleimide, used to suppress biothiol activity) exhibited strong fluorescence upon incubation with the  $F_{11}-Cu^{2+}$  complex (Fig. 17b).<sup>59</sup>

Xiaoming Feng and his research team reported a fluorescent compound,  $F_{12-a}$ , which, after reacting with  $Cu(NO_3)_2$ , functioned as a sensor for Cys, Hcy, and GSH through a fluorescence OFF–ON mechanism. Initially,  $F_{12-a}$  showed fluorescence quenching upon the addition of  $Cu(NO_3)_2$  in a 1 : 1 molar ratio. NMR and MS spectral analyses revealed that complex formation was accompanied by the oxidation of  $F_{12-a}$  into  $F_{12}$ . However, the exact oxidation state of copper in the complex was not identified; therefore, the complex was designated as  $F_{12}-Cu^{x+}$ . The  $F_{12}-Cu^{x+}$  acted as a selective fluorescent sensor for detecting Cys, Hcy, and GSH even in the presence of various non-thiol amino acids, *via* a ligand-exchange-induced fluorescence restoration process (Fig. 18).<sup>60</sup>

According to the published literature gathered to date, most fluorescent sensors that detect biothiols *via* this mechanism cannot differentiate between individual biothiols, likely due to the structural similarity and similar complexation ability of biothiols with metal ions. One of the very few fluorescent sensors operating by this mechanism that is capable of detecting Cys in the presence of GSH and Hcy was reported by Partha Pratim Parui and co-authors in *New J. Chem.* in 2017. In this work, the authors reported a fluorescent sensor based on the complex  $(F_{13})_2-(Cu^{2+})_3$ , which was formed between  $Cu^{2+}$  ions and the fluorescent compound  $F_{13}$  at a molar ratio of 3 : 2, and was able to selectively detect Cys at pH 7.4, even in the presence of biologically important molecules, including GSH and Hcy (Fig. 19a). The reason why this sensor exhibits selective

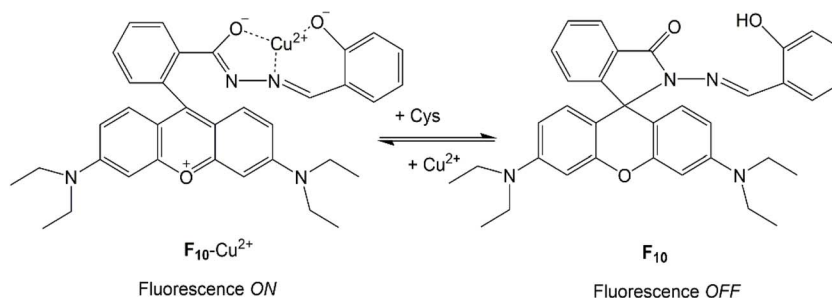


Fig. 16 The sensing mechanism of  $F_{10}-Cu^{2+}$  for Cys,<sup>58</sup> redrawn based on data reported in ref. 58, X.-F. Yang, P. Liu, L. Wang and M. Zhao, *J. Fluor.*, 2008, 18, 453–459, copyright 2008.



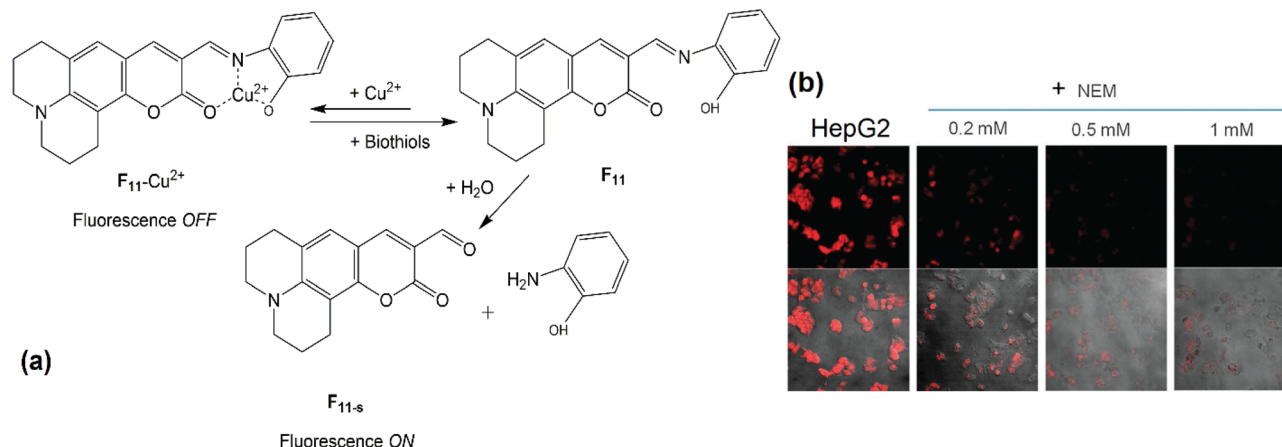


Fig. 17 (a) Fluorescence OFF–ON mechanism of the  $F_{11}\text{-Cu}^{2+}$  sensor upon reaction with biothiols, and (b) its application for detecting GSH in HepG2 cells,<sup>59</sup> adapted from ref. 59 with permission from the Royal Society of Chemistry, H. S. Jung, J. H. Han, Y. Habata, C. Kang and J. S. Kim, *Chem. Commun.*, 2011, 47, 5142–5144, copyright 2011.

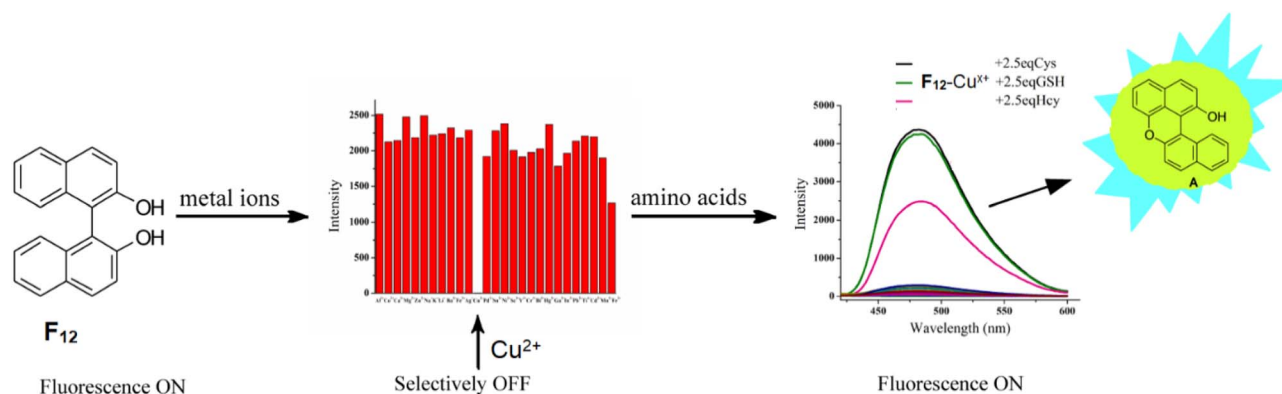


Fig. 18 The sensing mechanism of  $F_{12}\text{-Cu}^{2+}$  for biothiols,<sup>60</sup> adapted with permission from ref. 60, P. Ruixue, L. Lili, W. Xiaoxia, L. Xiaohua and F. Xiaoming, *J. Org. Chem.*, 2013, 78, 11602–11605. Copyright 2013 American Chemical Society.

reactivity towards Cys over GSH and Hcy is attributed to the difference in the acid dissociation constants ( $pK_a$ ) of the S–H groups, which directly interact with  $\text{Cu}^{2+}$  ions to form a new complex and release free  $F_{13}$ . Specifically, the  $pK_a$  values of the S–H groups in Cys, GSH, and Hcy are 8.15, 9.65, and 10.00, respectively. Therefore, at pH 7.4, the S–H group in Cys is partially deprotonated, allowing a stronger electrostatic interaction with  $\text{Cu}^{2+}$  ions compared to GSH and Hcy. However, the decomposition mechanism of the  $(F_{13})_2(\text{Cu}^{2+})_3$  complex by Cys was proposed to proceed through multiple complicated stages, including redox processes (Fig. 19b).<sup>61</sup>

Similarly, in another study, an  $F_{14}\text{-Cu}^{2+}$  complex was developed by coordinating  $\text{Cu}^{2+}$  with a coumarin-derived fluorescent compound ( $F_{14}$ ) at a 1 : 1 molar ratio (Fig. 20). This complex also enabled selective detection of Cys in the presence of various amino acids, as well as GSH and Hcy, in a  $\text{CH}_3\text{CN}/\text{HEPES}$  (7/3, v/v, pH 7.4) solution. The Cys selectivity was again attributed to the differences in the  $pK_a$  values of the –SH groups. Furthermore, the research group suggested that the –SH group in Cys experiences lower steric hindrance than those in GSH and Hcy,

thereby promoting a more favorable and selective interaction between Cys and  $\text{Cu}^{2+}$  ions.<sup>62</sup>

David G. Churchill and his co-authors reported a fluorescent sensor based on the  $F_{15}\text{-Cu}^{2+}$  complex. The sensing mechanism was proposed to involve the reduction of the metal center in the  $F_{15}\text{-Cu}^{2+}$  complex by cysteine, followed by imine bond hydrolysis, which led to fluorescence enhancement (Fig. 21). The detection limit for Cys was estimated to be  $6\ \mu\text{M}$ , which aligns with its physiological concentration. Notably, the sensor exhibited high selectivity for Cys over GSH, Hcy, acetyl-cysteine, methionine, and various other amino acids in a  $\text{CH}_3\text{OH}/\text{HEPES}$  buffer solution (30/70, v/v, pH 6.5). However, the underlying cause of this selectivity toward Cys over other thiols was not addressed in the study.<sup>63</sup>

**3.1.2 Complexes of  $\text{Cu}^{2+}$  with biothiols.** The reaction between metal ions and biothiols directly affects the equilibrium of the reaction between the sensor (a metal ion complex with a fluorophore) and biothiols. Therefore, studies on the complexes of metal ions with biothiols are of great importance.





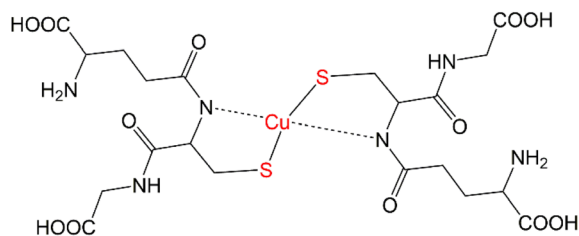


Fig. 22 The structure of the  $\text{Cu}^{2+}$ -GSH complex with a 1 : 2 molar ratio,<sup>64</sup> redrawn based on data reported in ref. 64.

The reaction between  $\text{Cu}^{2+}$  ions and GSH in solution was extensively investigated and also reported to be complex. According to existing literature, in the absence of oxygen or other oxidizing agents, the reaction between  $\text{Cu}^{2+}$  ions and GSH proceeded through the formation of Cu-S bridged complexes, initially with a  $\text{Cu}^{2+}$  : GSH molar ratio of 1 : 1, followed by 1 : 2 (reaction (1) Fig. 23).<sup>65</sup> When GSH was present in excess (GSH :  $\text{Cu}^{2+} \geq 3$  : 1),  $\text{Cu}^+[\text{GSH}]_2$  and GSSG were rapidly formed (reaction (2), Fig. 23).<sup>66-68</sup>

In the presence of oxygen or other oxidizing agents, such as free radicals generated during in physiological processes,  $\text{Cu}^{2+}$  catalyzed the oxidation of GSH to GSSG (Fig. 24). The mechanism of this process was proposed to proceed through reaction

pathways (4) and (5),<sup>65</sup> (6) and (7),<sup>69</sup> or (8) and (9).<sup>70</sup> The GSSG product also reacted with  $\text{Cu}^{2+}$  ions to form complexes. Eleven distinct complex structures were identified, among which the  $\text{Cu}_3[\text{GSSG}]_2^{2-}$  complex exhibited a logarithm of the equilibrium constant as high as 32.74.<sup>71</sup> The  $\text{Cu}^+$  intermediate also reacted with GSH to form stable complexes, with six structures reported. Among them, the  $\text{Cu}^+[(\text{GSH})\text{H}_2]_2^{3-}$  complex was the predominant species, showing a logarithm of the stability constant of 38.86.<sup>66</sup> However, studies also demonstrated that even in the presence of oxygen and  $\text{Cu}^{2+}$ , when EDTA – a strong  $\text{Cu}^{2+}$  chelator – was added, the GSH concentration remained nearly unchanged after 3 hours of exposure to oxygen.<sup>65</sup>

In summary, current studies suggested that the interaction between  $\text{Cu}^{2+}$  ions and GSH in solution was quite complex. Initially, the  $\text{Cu}^{2+}(\text{GSH})_2$  complex was formed, and in the presence of excess GSH (at a GSH :  $\text{Cu}^{2+}$  ratio equal to or greater than 3 : 1) or oxidizing agents, GSH was oxidized to GSSG, which subsequently formed complexes with  $\text{Cu}^{2+}$ . No studies had precisely determined the structure of the  $\text{Cu}^{2+}(\text{GSH})_2$  complex in solution or its stability constant. This information was essential for evaluating the potential exchange reaction between the  $\text{Cu}^{2+}$ -fluorophore complex and GSH, as well as the competitive interactions among biothiols.

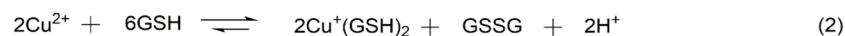
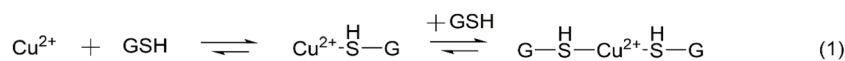


Fig. 23 Reaction between  $\text{Cu}^{2+}$  ions and GSH under non-oxidizing conditions.

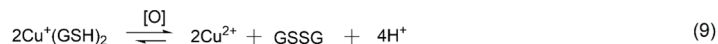
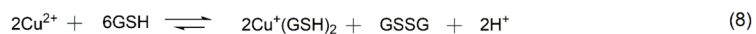
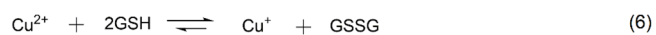
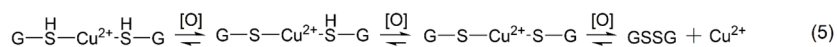
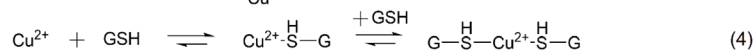


Fig. 24 Reaction between  $\text{Cu}^{2+}$  ions and GSH in the presence of oxidizing agents.

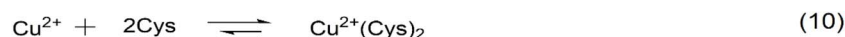


Fig. 25 Reaction between  $\text{Cu}^{2+}$  ions and Cys,<sup>56,61,73</sup> redrawn based on data reported in ref. 56, 61 and 73.



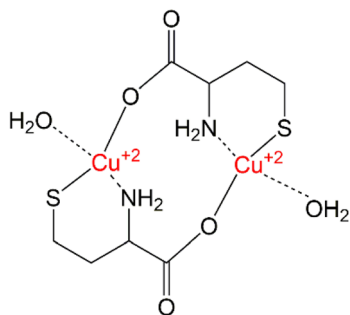


Fig. 26 The structure of the  $(\text{Cu}^{2+})_2(\text{Hcy})_2(\text{H}_2\text{O})_2$  complex,<sup>74</sup> redrawn based on data reported in ref. 74.

**3.1.2.2 The reaction between  $\text{Cu}^{2+}$  ions and Cys.** The reaction between  $\text{Cu}^{2+}$  ions and Cys depended on the solvent used. In ethanol, Jorge L. Gardea-Torresdey and co-authors successfully synthesized  $\text{Cu}^{2+}$ -Cys complexes with molar ratios of 1 : 2, 1 : 4, and 1 : 6, which formed monoclinic cage-like clusters based on Cu-S coordination. In these complexes, copper was identified as remaining in the  $\text{Cu}^{2+}$  oxidation state.<sup>72</sup>

At first,  $\text{Cu}^{2+}$  reacted with Cys to form the  $\text{Cu}^{2+}(\text{Cys})_2$  complex (reaction (10)) (Fig. 25), whose stability constant was determined to be 10.<sup>16</sup> Simultaneously, a redox process occurred, in which Cys was oxidized to cystine (CSSC) and  $\text{Cu}^{2+}$  was reduced to  $\text{Cu}^+$  (reaction (11)). The generated  $\text{Cu}^+$  ions then reacted with

CSSC to form the  $\text{Cu}^+$ -CSSC complex (reaction (12)), while  $\text{Cu}^+$  also reacted with Cys to form the  $\text{Cu}^+$ -Cys complex (reaction (13)), whose stability constant was reported as 10.<sup>19</sup> In addition,  $\text{Cu}^+$  ions could be oxidized back to  $\text{Cu}^{2+}$  by oxygen or other oxidizing agents (reaction (14)).<sup>56,61,73</sup>

**3.1.2.3 The reaction between  $\text{Cu}^{2+}$  ions and Hcy.** Analogous to GSH and Cys, the reaction between  $\text{Cu}^{2+}$  ions and homocysteine (Hcy) in aqueous solution resulted in the formation of complexes and/or redox transformations, depending on the specific reaction conditions. In neutral aqueous medium, when  $\text{Cu}^{2+}$  and Hcy were present in a 1 : 1 molar ratio, a blue-colored complex, identified as  $(\text{Cu}^{2+})_2(\text{Hcy})_2(\text{H}_2\text{O})_2$  (Fig. 26), was characterized. In contrast, under excess Hcy conditions (where the concentration of Hcy was more than three times that of  $\text{Cu}^{2+}$ ), an insoluble yellow complex, attributed to the interaction between  $\text{Cu}^+$  and Hcy ( $\text{Cu}^+$ -Hcy), was formed. Notably, this  $\text{Cu}^+$ -Hcy complex could also be generated by thermal decomposition of the aforementioned blue complex. In the presence of oxygen or other oxidizing agents,  $\text{Cu}^+$  was readily reoxidized to  $\text{Cu}^{2+}$ . Based on these observations, the overall redox process between  $\text{Cu}^{2+}$  and Hcy was proposed as illustrated in Fig. 27.<sup>74</sup>

Previous studies also showed that, under neutral, physiological, and human plasma conditions, Hcy exhibited distinct redox properties compared to other thiols such as GSH and Cys. This difference arose from the formation of  $\alpha$ -radicals during oxidation, wherein the thyl radicals underwent hydrogen atom

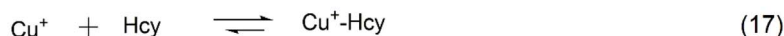
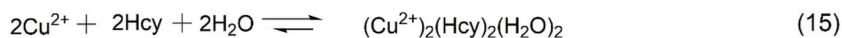


Fig. 27 Reaction between  $\text{Cu}^{2+}$  ions and Hcy,<sup>74</sup> redrawn based on data reported in ref. 74.

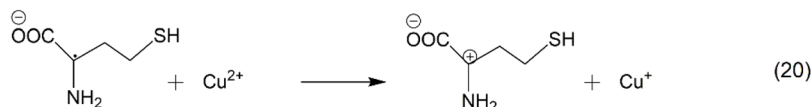
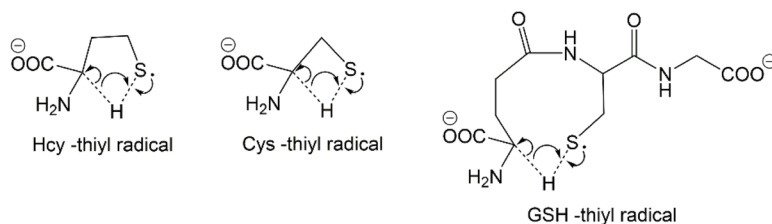
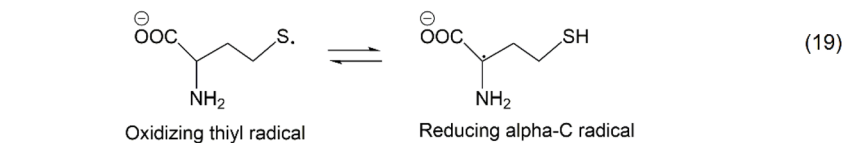


Fig. 28 Redox interconversion between thyl and  $\alpha$ -radicals in thiols,<sup>75</sup> redrawn based on data reported in ref. 75.





Table 4 Summary of fluorescence sensors for biothiol detection based on metal ion complexation/decomplexation reactions

Sensors	Dissociation constant	Detectable biothiols	LOD $\mu\text{M}$	Solvent/pH	[Biothiols]/ $[\text{M}^{\text{tr}}]_{\text{f}}$	Application/note	Ref.
<b>F<sub>1</sub>-Cu<sup>2+</sup></b>	None	GSH Cys	0.16	HEPES/DMSO (95/5, v/v), pH 7.4	3/1	Detect biothiols in live cells	39
<b>F<sub>2</sub>-Cu<sup>2+</sup></b>	$6.29 \times 10^{-6}$	Hcy	0.80	DMF/HEPES (3/7, v/v), pH 7.4	4/3	Detect biothiols in the human lung cancer cell A549	40
		GSH	1.00				
		Hcy	1.50				
<b>F<sub>3</sub>-Cu<sup>2+</sup></b>	$6.92 \times 10^{-8}$	GSH	0.30	Ethanol/HEPES (1/1, v/v), pH 7.4	2/1	None	19
		Cys					
		Hcy					
<b>F<sub>4</sub>-Cu<sup>2+</sup></b>	$6.25 \times 10^{-6}$	GSH	0.17	CH <sub>3</sub> CN/HEPES (1/1, v/v), pH 7.4	None	The influence of GSH was not investigated	52
		Cys	0.25				
		Hcy	None				
<b>F<sub>5</sub>-Cu<sup>2+</sup></b>	$7.56 \times 10^{-6}$	GSH	None	CH <sub>3</sub> OH/HEPES (1/1, v/v), pH 7.4	6/1	None	53
		Cys					
		Hcy					
<b>F<sub>6</sub>-Cu<sup>2+</sup></b>	$26.5 \times 10^{-6}$	GSH	0.20	CH <sub>3</sub> OH/HEPES (9/1, v/v), pH 7.2	None	Detect GSH in HeLa cells	54
		Cys					
		Hcy					
<b>(F<sub>7</sub>)<sub>2</sub>-Cu<sup>2+</sup></b>	$1.37 \times 10^{-8}$	GSH	0.44	DMF/HEPES (7 : 3, v/v), pH 7.4	$\approx 3.5/1$ $\approx 7.0/1$	Detect biothiols in human urine samples	55
		Cys	0.96				
		Hcy	0.68				
<b>(F<sub>8</sub>)<sub>3</sub>-(Cu<sup>2+</sup>)<sub>2</sub></b>	None	GSH	None	DMSO	None	None	56
		Cys					
		Hcy					
<b>F<sub>9</sub>-(Cu<sup>2+</sup>)<sub>2</sub></b>	$0.13 \times 10^{-6}$	GSH	None	0.1 M NaCl, 0.05 M HEPES, pH 7	None	None	57
		Cys					
		Hcy					
<b>F<sub>10</sub>-Cu<sup>2+</sup></b>	None	Cys	0.14	C <sub>2</sub> H <sub>5</sub> OH/H <sub>2</sub> O (4/6, v/v), Tris-HCl, pH 7.1	None	The influence of GSH and Hcy was not investigated	58
		GSH	0.01				
		Cys					
<b>F<sub>11</sub>-Cu<sup>2+</sup></b>	None	GSH	None	10 mM PBS buffer, pH, 7.4, 1% DMSO	None	Detect biothiols in HepG2 cells	59
		Cys					
		Hcy					
<b>F<sub>12</sub>-Cu<sup>2+</sup></b>	None	GSH	None	CH <sub>3</sub> CN/H <sub>2</sub> O (1/1, v/v)	None	None	60
		Cys					
		Hcy					
<b>(F<sub>13</sub>)<sub>2</sub>-(Cu<sup>2+</sup>)<sub>3</sub></b>	None	Cys	1.0	20 mM HEPES-NaOH, pH, 7.4	60/1	Detect Cys in multicellular <i>Caenorhabditis elegans</i>	61
		GSH	0.015				
		Cys	6.0				
<b>F<sub>14</sub>-Cu<sup>2+</sup></b>	$0.50 \times 10^{-6}$	Cys	0.015	CH <sub>3</sub> CN/HEPES (7/3, v/v), pH 7.4	2/1	Detect Cys in live A549 cells	62
		GSH	6.0				
		Cys	6.0				
<b>F<sub>15</sub>-Cu<sup>2+</sup></b>	$1.67 \times 10^{-6}$	Cys	6.0	CH <sub>3</sub> OH/HEPES (3/7, v/v), pH 6.5	30/1	None	63
		GSH	0.016				
		Cys	0.0002				
<b>(K<sub>2</sub>)<sub>2</sub>-(Hg<sup>2+</sup>)<sub>2</sub></b>	$3.57 \times 10^{-18}$	GSH	0.0002	Ethanol/HEPES (1/9, v/v), pH 7.4	2/1	The influence of GSH and Hcy was not investigated	82
		Cys					
		Hcy					
<b>K<sub>3</sub>-Hg<sup>2+</sup></b>	$50.5 \times 10^{-6}$	GSH	0.0001	Water (1%DMSO), HEPES, pH 7.4	$\approx 9/1$	Detect Cys in <i>Candida albicans</i> cells	83
		Cys					
		Hcy					
<b>K<sub>4</sub>-Hg<sup>2+</sup></b>	$90.1 \times 10^{-6}$	GSH	0.07	THF	2/1	GSH and Hcy could react in a similar manner to Cys	84
		Cys					
		Hcy					

Table 4 (Contd.)

Sensors	Dissociation constant	Detectable biothiols	LOD $\mu\text{M}$	Solvent/pH	[Biothiols]/ $[\text{M}^{n+}]^a$	Application/note	Ref.
$(\text{K}_5)_2\text{-Hg}^{2+}$	$0.4 \times 10^{-12}$	GSH	0.34	Water, in pH 7.2 phosphate buffer	2/1	None	85
		Cys	0.47				
		Hcy	0.26				
$\text{K}_6(\text{Hg}^{2+})_2$	$1.72 \times 10^{-4}$	GSH	0.0138	HEPES/DMSO (v/v, 95/5)	2/1	Detect biothiols in HepG2 cells	86
		Cys	0.0130				
		Hcy	0.0146				
$\text{K}_7\text{-Hg}^{2+}$	$0.25 \times 10^{-6}$	GSH	0.3	10 mM HEPES buffer, pH 7.4 containing 5% $\text{CH}_3\text{CN}$	1/1	The influence of Hcy was not investigated. Detect GSH in human serum and FBS	87
		Cys	0.029				
$(\text{K}_8)_2\text{-Hg}^{2+}$	$4.90 \times 10^{-6}$	Cys	0.029	DMF/HEPES (1 : 9, v/v) pH 8.0	2/1	GSH and Hcy had no effect adding excess Cys to $(\text{K}_8)_2\text{-Hg}^{2+}$ yields the complex $(\text{Cys})_4\text{Hg}^{2+}$	88
		GSH	$16 \times 10^{-9}$				
$\text{L}_1\text{-Fe}^{3+}$	$4.81 \times 10^{-5}$	Cys	0.446	Water (1% DMSO) pH: 2-11	1/1	GSH and Hcy had no effect	94
$\text{M}_1\text{-Ag}^+$	$5.29 \times 10^{-6}$	GSH	0.208				
		Cys	0.089				
		Hcy	0.174				

<sup>a</sup> [Biothiols]/ $[\text{M}^{n+}]$ : the concentration ratio of [biothiols]/[metal ion] required to fully restore the fluorescence intensity of the  $\text{F}_1\text{-M}^{n+}$  complex solution, resulting in a fluorescence intensity equal to that of the free  $\text{F}_1$  solution. None: not investigated or not reported.

transfer (HAT) to generate transition states. Notably, Hcy was capable of forming a five-membered cyclic transition state that was kinetically more favorable than those formed by GSH or Cys. This explained the observed difference during the reflux of  $\text{Cu}^{2+}$  solutions with Hcy, Cys, and GSH, where only Hcy induced the reduction of  $\text{Cu}^{2+}$  to  $\text{Cu}^+$ , leading to a visible color change in the solution. The selectivity was attributed to the strong reducing nature of the  $\text{C}\alpha$ -radical ( $E^0(\text{NH}_2 = \text{CHR}^+/\text{NH}_2\text{CHR}) = -1.9 \text{ V vs. NHE}$ ), in contrast to the oxidizing character of the thiyl radical ( $E^0(\text{RS}^\cdot, \text{H}^+/\text{RSH}) = +1.3 \text{ V vs. NHE}$ ) (Fig. 28). This unique reactivity was exploited by several researchers to achieve selective detection of Hcy in the presence of GSH and Cys in neutral buffer and blood plasma using mild redox-active chromogenic agents such as methyl viologen.<sup>75-81</sup>

**3.1.3 Summary of fluorescent sensors for biothiol detection based on  $\text{Cu}^{2+}$  complexes.** In summary, recent studies demonstrated that sensors based on complexes of fluorescent ligands with  $\text{Cu}^{2+}$  were effective tools for detecting biothiols in the presence of various non-thiol amino acids, with reported detection limits as low as  $0.015 \mu\text{M}$  (Table 4). The sensing mechanism typically involved an initial ligand exchange between  $\text{Cu}^{2+}$  and the biothiol, resulting in the release of a free fluorophore that served as the quantifiable signal. This was followed by redox reactions between  $\text{Cu}^{2+}$  and the biothiol, as well as the formation of intermediate complexes. Subsequently, the oxidation of  $\text{Cu}^+$  regenerated  $\text{Cu}^{2+}$ , which can rebind to the original fluorophore. These interrelated processes highlighted key considerations in the design of new sensors, particularly with respect to their response time and reversibility.

However, due to the high structural similarity among biothiols, most sensors that employed this mechanism could not effectively discriminate between GSH, Cys, and Hcy. Some sensors, such as  $(\text{F}_{13})_2\text{-}(\text{Cu}^{2+})_3$ ,  $\text{F}_{14}\text{-Cu}^{2+}$ , and  $\text{F}_{15}\text{-Cu}^{2+}$ , demonstrated selective detection of Cys in the presence of GSH and Hcy, a result commonly attributed to differences in the  $\text{pK}_a$  values of the thiol groups (8.15 for Cys, 9.65 for GSH, and 10.00 for Hcy).<sup>61,62</sup> However, this explanation proved unconvincing. For instance, when comparing  $\text{F}_2\text{-Cu}^{2+}$  and  $\text{F}_4\text{-Cu}^{2+}$  with  $\text{F}_{14}\text{-Cu}^{2+}$  under identical pH conditions (pH = 7.4), and given that their dissociation constants differed only slightly ( $6.92 \times 10^{-6}$ ,  $6.25 \times 10^{-6}$ , and  $0.5 \times 10^{-6}$ , respectively),  $\text{F}_2\text{-Cu}^{2+}$  and  $\text{F}_4\text{-Cu}^{2+}$  failed to differentiate Cys from GSH and Hcy, whereas  $\text{F}_{14}\text{-Cu}^{2+}$  succeeded (Table 4). A more plausible explanation lay in steric effects, which might have influenced the accessibility and coordination ability of specific thiols toward the metal center, offering a promising avenue for enhancing selectivity in future sensor design.<sup>62</sup>

Another potential avenue for sensor development involved exploiting the differences in the stability and redox behavior of  $\text{C}\alpha$ -radicals derived from different biothiols. Free fluorophores released upon ligand exchange with  $\text{Cu}^{2+}$  could serve as mild oxidants capable of selectively reacting with such radicals, particularly those of homocysteine, which was known to form a kinetically favorable five-membered cyclic transition state. This unique reactivity opened up new opportunities to design next-generation  $\text{Cu}^{2+}$ -based sensors with improved selectivity and sensitivity for targeted biothiol species in complex biological environments such as blood plasma.



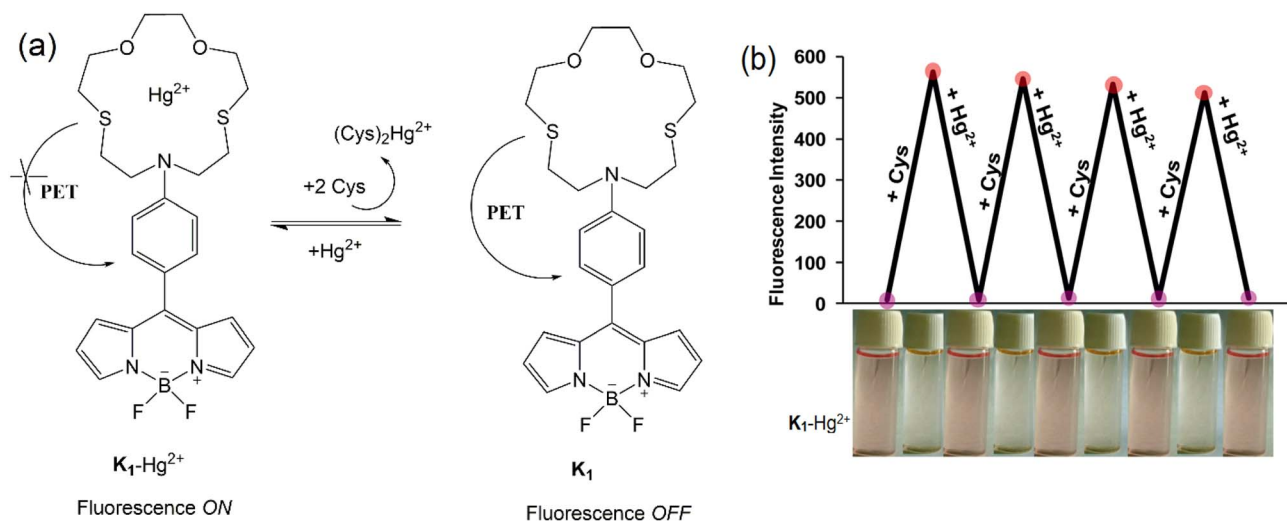


Fig. 29 (a) Fluorescence ON–OFF sensing of Cys by the  $K_1$ - $Hg^{2+}$  complex; (b) fluorescence changes upon sequential addition of Cys and  $Hg^{2+}$  ions,<sup>82</sup> adapted from ref. 82 with permission from the Royal Society of Chemistry, N. Kaur, P. Kaur and K. Singh, *RSC Adv.*, 2014, 4, 29340–29343, copyright 2014.

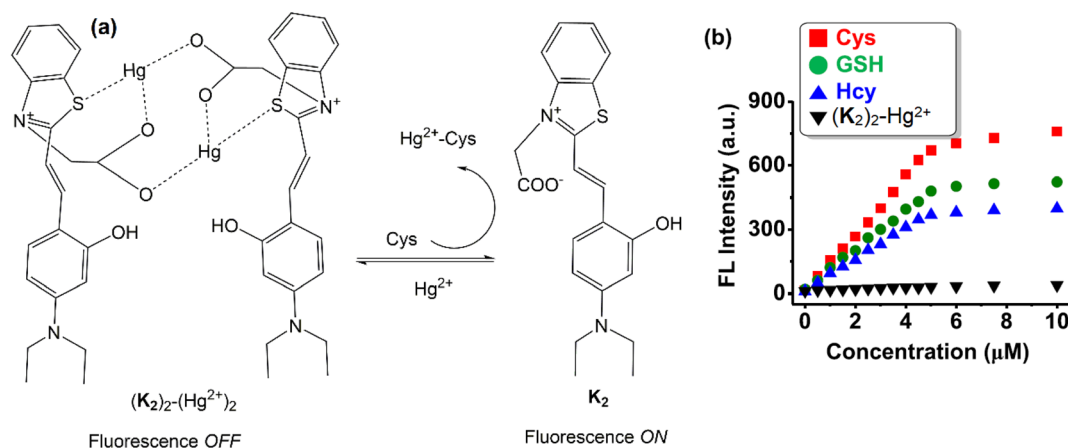


Fig. 30 (a)  $(K_2)_2-(Hg^{2+})_2$ -based fluorescent sensor for Cys, (b) fluorescence changes upon incremental addition of GSH, Cys, and Hcy,<sup>20</sup> adapted from ref. 20, D. T. Nhan, N. K. Hien, H. Van Duc, N. T. A. Nhung, N. T. Trung, D. U. Van, W. S. Shin, J. S. Kim and D. T. Quang, *Dyes Pigment.*, 2016, 131, 301–306. Copyright 2016, with permission from Elsevier.

### 3.2 Sensors based the on complexation/decomplexation of $Hg^{2+}$ ions

**3.2.1 Sensors based on  $Hg^{2+}$  complexes.** Following  $Cu^{2+}$  complexes, fluorescent sensors for biothiols that employed  $Hg^{2+}$  complexes were also widely reported. A fluorescent sensor for detecting Cys, based on the  $K_1$ - $Hg^{2+}$  complex formed between compound  $K_1$  and  $Hg^{2+}$  in a 1:1 molar ratio, operating *via* a fluorescence ON–OFF mechanism, was reported by Navdeep Kaur and co-authors (Fig. 29a). In its free state,  $K_1$  exhibited weak fluorescence due to the PET process occurring from the dioxadithiaazacrown ether moiety to the BODIPY unit. In the  $K_1$ - $Hg^{2+}$  complex, interactions between  $Hg^{2+}$  and the dioxadithiaazacrown ether moiety suppressed this PET process, leading to strong fluorescence emission of the  $K_1$ - $Hg^{2+}$  complex at 520 nm. This method allowed Cys detection in the presence

of non-thiol amino acids with a detection limit of 0.016  $\mu M$ , and the sensor remained reusable for at least five detection cycles (Fig. 29b). The study also confirmed the structure of the complex between Cys and  $Hg^{2+}$  as  $(Cys)_2Hg^{2+}$  based on experimental spectral data. However, a limitation was that the study did not investigate the influence of other thiols such as GSH and Hcy.<sup>82</sup>

Nhan and co-authors introduced a complex of  $Hg^{2+}$  with the fluorescent compound  $K_2$ , structured as  $(K_2)_2-(Hg^{2+})_2$ , which was capable of detecting biothiols in an ethanol/HEPES solution (1/9, v/v, pH = 7.4) in the presence of various competing amino acids such as Ala, Asp, Arg, Gly, Glu, Ile, Leu, Lys, Met, Thr, Ser, Tyr, Trp, Val, and His (Fig. 30). Biothiols reacted with the  $(K_2)_2-(Hg^{2+})_2$  complex, releasing free  $K_2$ , resulted in an increase in fluorescence intensity at 585 nm (excitation wavelength at 540 nm). The fluorescence intensity of the  $(K_2)_2$ -



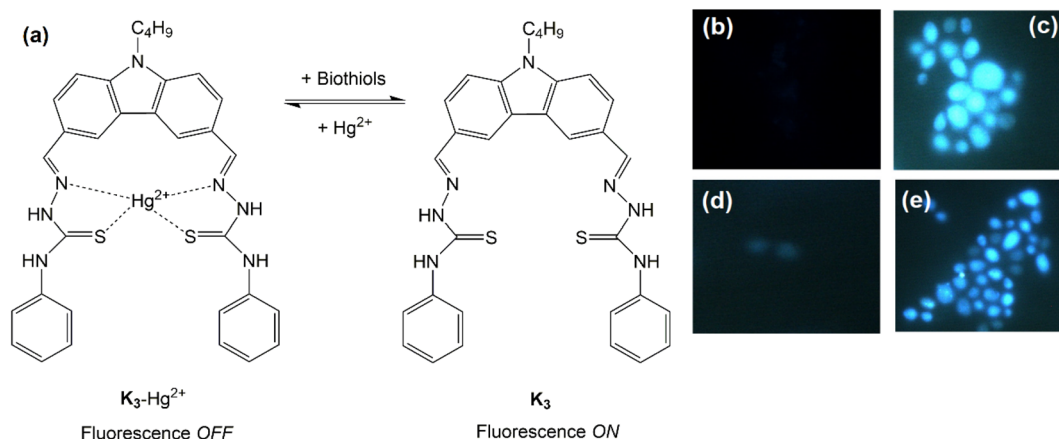


Fig. 31 (a)  $K_3$ - $Hg^{2+}$  sensor for biothiols, (b–e) fluorescence microscopy images: (b) *Candida albicans* cells only, (c) *Candida albicans* +  $K_3$ , (d) *Candida albicans* +  $K_3$ - $Hg^{2+}$ , (e) *Candida albicans* +  $K_3$ - $Hg^{2+}$  + Cys,<sup>83</sup> adapted from ref. 83, A. K. Mahapatra, J. Roy, P. Sahoo, S. K. Mukhopadhyay, A. Banik and D. Mandal, *Tetrahedron Lett.*, 2013, 54, 2946–2951. Copyright 2013, with permission from Elsevier.

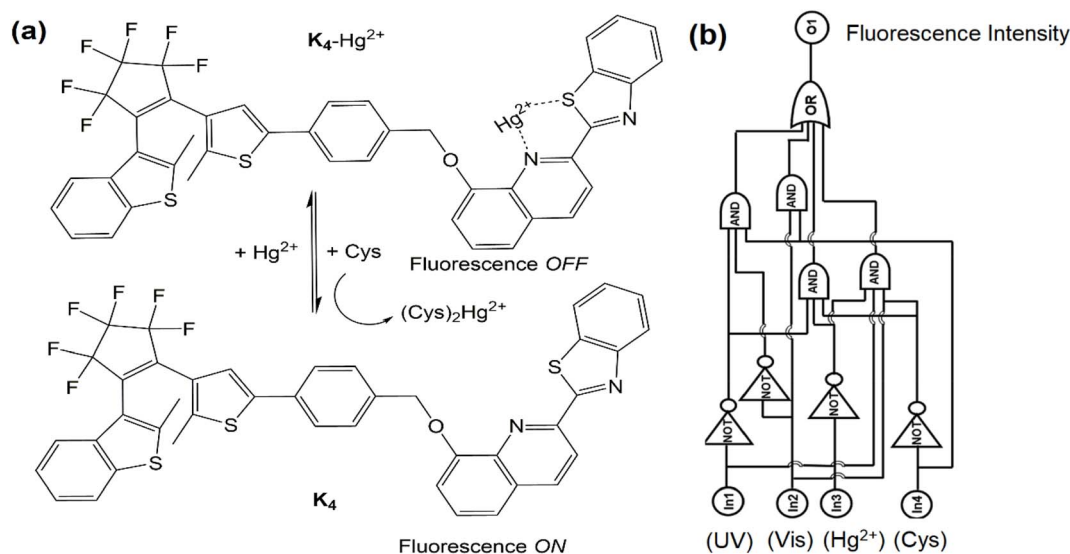


Fig. 32 (a) Fluorescent OFF–ON sensor for Cys based on the  $Hg^{2+}$  complex of a diarylethene derivative ( $K_4$ - $Hg^{2+}$ ), and (b) logic circuit showing the relationship between the input signals (UV, Vis,  $Hg^{2+}$ , and Cys) and the output signal (fluorescence intensity),<sup>84</sup> adapted from ref. 84, *RSC Adv.*, 2017, 7, 20591–20596, copyright 2017, The Royal Society of Chemistry. Licensed under a Creative Commons Attribution-NonCommercial 3.0 Unported Licence.

( $Hg^{2+}$ )<sub>2</sub> solution nearly recovered to that of free  $K_2$  when the biothiol concentration was equivalent to the initial concentration of  $Hg^{2+}$  in the complex solution. The ( $K_2$ )<sub>2</sub>-( $Hg^{2+}$ )<sub>2</sub> complex exhibited sensitivity toward biothiols in the order of Cys > GSH > Hcy. The detection limit for Cys by the ( $K_2$ )<sub>2</sub>-( $Hg^{2+}$ )<sub>2</sub> complex was determined to be 0.2 nM, which was significantly lower than the normal human intracellular Cys concentration (30–200  $\mu$ M). This sensor was also shown to operate for at least five cycles of alternating additions of Cys/ $Hg^{2+}$  concentrations, demonstrating its potential for reuse in detecting Cys in various subjects.<sup>20</sup>

A 1 : 1 molar complex that was formed between the fluorophore  $K_3$  and  $Hg^{2+}$  ions was reported as a fluorescent sensor for detecting biothiols. GSH, Hcy, and Cys reacted with the  $K_3$ - $Hg^{2+}$

complex, releasing free  $K_3$  and restoring fluorescence (Fig. 31a). Other amino acids did not affect the fluorescence signal of the  $K_3$ - $Hg^{2+}$  complex solution. Among the biothiols, Cys induced the highest fluorescence recovery. When a solution containing 5  $\mu$ M of the  $K_3$ - $Hg^{2+}$  complex was used, a Cys concentration of up to 45  $\mu$ M was required to achieve maximum fluorescence recovery. The linear range for quantifying Cys was determined to be 0.5–30  $\mu$ M, with a detection limit of  $9.6 \times 10^{-5}$   $\mu$ M. The complex between Cys and  $Hg^{2+}$  was suggested to exist in the form of  $Hg(Cys)_2$ , as previously described. The  $K_3$ - $Hg^{2+}$  sensor was successfully applied to detect Cys in *Candida albicans* cells using fluorescence microscopy imaging (Fig. 31b).<sup>83</sup>

Another sensor based on a complex between  $Hg^{2+}$  and a fluorescent compound derived from diarylethene and



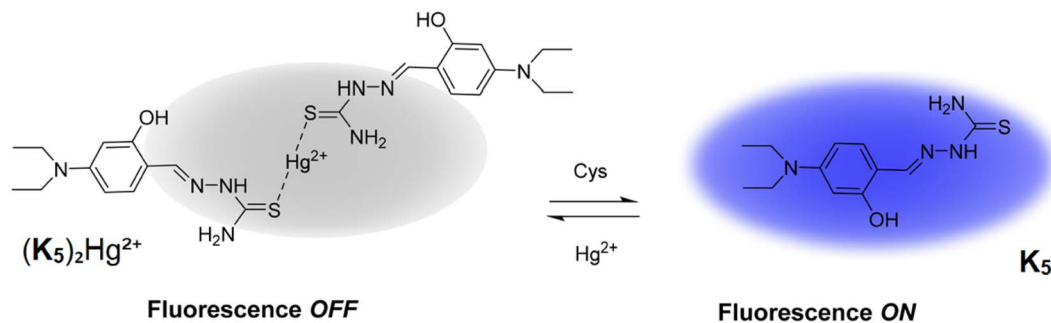


Fig. 33 Sensor for biothiol detection based on the  $\text{Hg}^{2+}$  complex of a 4-(diethylamino)salicylaldehyde derivative ( $\text{K}_5$ ),<sup>85</sup> reproduced from ref. 85, N. K. Hien, T. T. G. Chau, N. D. Luyen, Q. V. Vo, M. Van Bay, S. T. Ngo, P. C. Nam & D. T. Quang, *RSC Adv.*, 2025, **15**, 20125–20133, copyright 2025, The Royal Society of Chemistry. Licensed under a Creative Commons Attribution 3.0 Unported Licence.

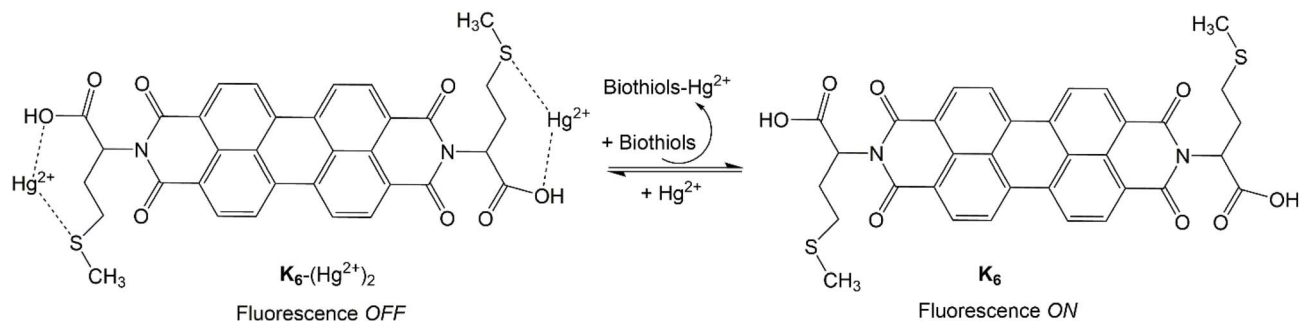


Fig. 34  $\text{Hg}^{2+}$  complex of a perylene bisimide derivative,  $\text{K}_6\text{-(Hg}^{2+})_2$ , used for biothiol detection *via* a complex-exchange mechanism,<sup>86</sup> redrawn based on data reported in ref. 86, Ş. N. Karuk Elmas, I. Berk Gunay, A. Karagoz, A. Bostanci, G. Sadi and I. Yilmaz, *Electroanalysis*, 2020, **32**, 775–780, copyright 2020.

quinoline ( $\text{K}_4$ ) was reported by Shouzhi Pu and his research team, which was capable of detecting Cys *via* a complexation/decomplexation mechanism (Fig. 32a). In THF solution, the free form of  $\text{K}_4$  exhibited strong fluorescence with a maximum emission at 468 nm.  $\text{Hg}^{2+}$  formed a 1 : 1 molar complex with  $\text{K}_4$ , leading to fluorescence quenching. The  $\text{K}_4\text{-Hg}^{2+}$  complex reacted with Cys to form a new  $(\text{Cys})_2\text{Hg}^{2+}$  complex and released free  $\text{K}_4$ , resulting in fluorescence restoration. As a result, the  $\text{K}_4\text{-Hg}^{2+}$  sensor was able to detect Cys in the presence of non-thiol amino acids, with a detection limit of 0.07  $\mu\text{M}$ . Although this study did not examine the influence of GSH and Hcy, other organic thiols such as ethylene mercaptan, 2-aminothiophenol, and 2-aminoethanethiol exhibited similar responses to that of Cys. These findings suggested that the sensor was likely unable to selectively distinguish Cys in the presence of GSH and Hcy. Based on the fact that the fluorescence of  $\text{K}_4$  could be effectively modulated by light irradiation and the chemical inputs  $\text{Hg}^{2+}$  and Cys, a logic circuit was also successfully constructed, employing fluorescence intensity as the output signal and UV/Vis light,  $\text{Hg}^{2+}$ , and Cys as the input signals (Fig. 32b). This finding indicated great potential for the future application of these sensors in important studies, particularly for continuous and online monitoring.<sup>84</sup>

A 2 : 1 molar ratio complex between  $\text{Hg}^{2+}$  and compound  $\text{K}_5$ , a derivative of 4-(diethylamino)salicylaldehyde and aminothio-urea, was reported by Nguyen Khoa Hien and co-authors as

a potential sensor for biothiols *via* a complex-exchange mechanism, exhibiting a fluorescence OFF–ON response (Fig. 33). The sensor  $(\text{K}_5)_2\text{-Hg}^{2+}$  was able to detect GSH, Cys, and Hcy in the presence of other non-thiol amine acids, with detection limits of 0.34, 0.47, and 0.26  $\mu\text{M}$ , respectively. The stability constant of the  $(\text{K}_5)_2\text{-Hg}^{2+}$  complex was determined to be  $10^{12.395}$ , which was significantly lower than those of the corresponding  $\text{HgL}_2$  complexes, where L represented GSH, Cys, or Hcy ( $10^{41.58}$ ,  $10^{43.57}$ , and  $10^{39.40}$ , respectively). Consequently, all three biothiols reacted with  $(\text{K}_5)_2\text{-Hg}^{2+}$ , releasing free  $\text{K}_5$ . Therefore, the  $(\text{K}_5)_2\text{-Hg}^{2+}$  sensor was unable to distinguish between GSH, Cys, and Hcy.<sup>85</sup>

Another fluorescent sensor for GSH, Cys, and Hcy based on the complex  $\text{K}_6\text{-(Hg}^{2+})_2$  was reported, in which the fluorophore  $\text{K}_6$  was a perylene bisimide derivative (Fig. 34). In a HEPES/DMSO solution (v/v, 95/5), the  $\text{K}_6\text{-(Hg}^{2+})_2$  complex reacted with GSH, Cys, and Hcy to release free  $\text{K}_6$ , accompanied by an OFF–ON fluorescence response. In contrast, other amino acids including Ala, Glu, Gly, His, Ile, Leu, Lys, Met, Phe, Pro, Ser, Trp, Val, Thr, and Asp did not affect the fluorescence signal of the  $\text{K}_6\text{-(Hg}^{2+})_2$  complex solution. Consequently, the  $\text{K}_6\text{-(Hg}^{2+})_2$  complex was applicable as a fluorescent sensor for detecting GSH, Cys, and Hcy in the presence of those amino acids, with detection limits of 13.8, 13.0, and 14.6 nM, respectively. The stability constant of the  $\text{K}_6\text{-(Hg}^{2+})_2$  complex was determined to be  $5.82 \times 10^3 \text{ M}^{-1}$ , was significantly lower than those of the complexes



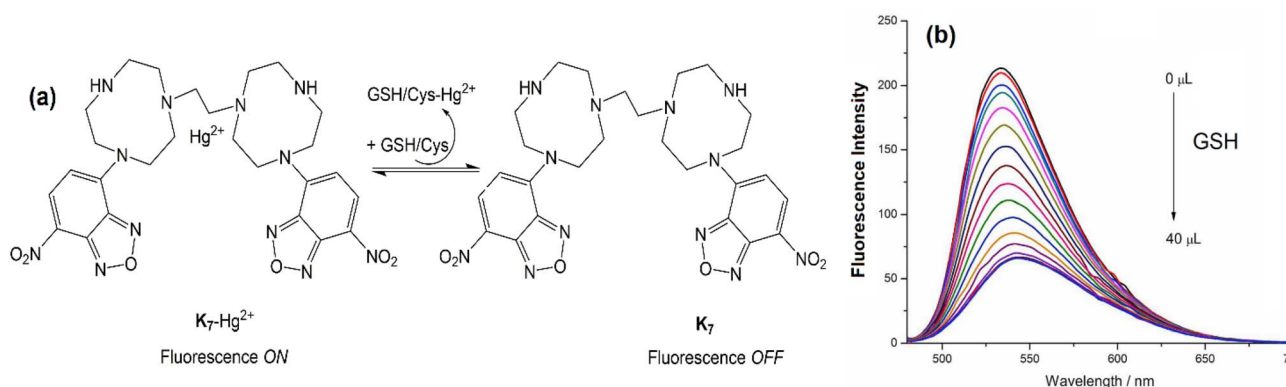


Fig. 35 (a) Fluorescence turn-on sensor  $K_7\text{-Hg}^{2+}$  for GSH/Cys detection, (b) fluorescence titration spectra of  $K_7\text{-Hg}^{2+}$  with GSH,<sup>87</sup> adapted from ref. 87, X. Wang, X. Ma, J. Wen, Z. Geng and Z. Wang, *Talanta*, 2020, **207**, 120311. Copyright 2020, with permission from Elsevier.

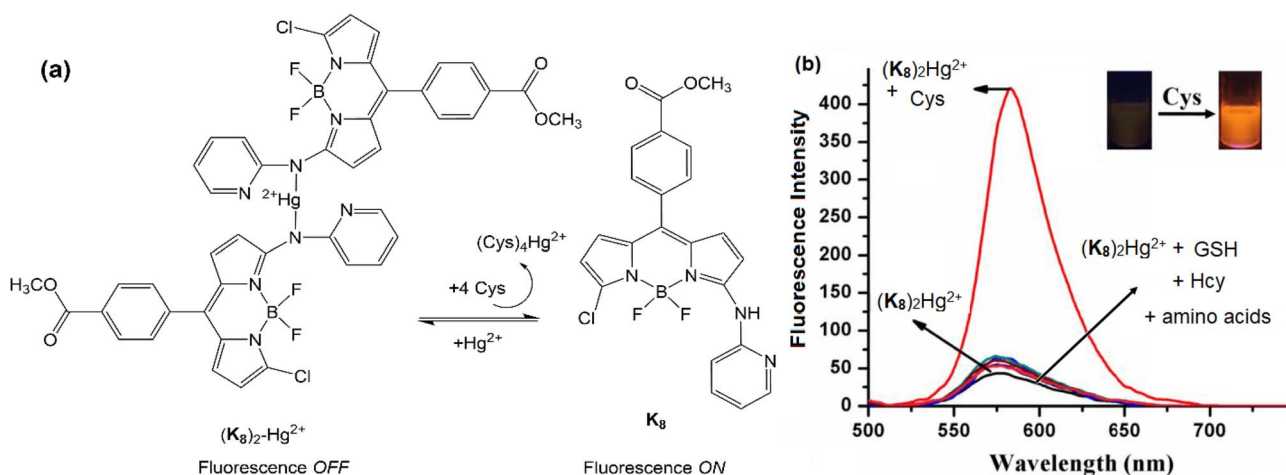


Fig. 36 (a)  $(K_8)_2\text{-Hg}^{2+}$  sensor for the selective detection of Cys, (b) fluorescence spectral changes of the sensor upon addition of Cys, GSH, Hcy, and various other amino acids,<sup>88</sup> adapted from ref. 88 with permission from the Chemical Society of Japan, published by Springer Nature, M. Kumar, G. Chaudhary and A. P. Singh, *Anal. Sci.*, 2021, **37**, 283–292, copyright 2021.

formed between  $\text{Hg}^{2+}$  and GSH, Cys, or Hcy. This likely accounted for the sensor's inability to distinguish among the three biothiols. The  $(K_6)_2\text{-Hg}^{2+}$  sensor was also successfully evaluated for its ability to detect biothiols in HepG2 cells using fluorescence imaging.<sup>86</sup>

One of the few reported fluorescent sensors for GSH/Cys based on a complex that operated *via* a fluorescence ON–OFF mechanism was the  $K_7\text{-Hg}^{2+}$  complex (Fig. 35). Unlike many previously reported sensors, the  $K_7\text{-Hg}^{2+}$  complex exhibited strong fluorescence at a maximum emission wavelength of 530 nm in a 10 mM HEPES buffer solution (pH 7.4) containing 5%  $\text{CH}_3\text{CN}$ . GSH and Cys reacted with the  $K_7\text{-Hg}^{2+}$  complex, resulting in the release of free  $K_7$  and a subsequent quenching of fluorescence. In contrast, various anions and amino acids such as  $\text{F}^-$ ,  $\text{Cl}^-$ ,  $\text{Br}^-$ ,  $\text{CH}_3\text{COO}^-$ ,  $\text{CO}_3^{2-}$ ,  $\text{NO}_3^-$ ,  $\text{PO}_4^{3-}$ ,  $\text{SO}_4^{2-}$ , PPI, glycine, histidine, aspartic acid, tyrosine, threonine, and GSSG did not affect the fluorescence signal of the  $K_7\text{-Hg}^{2+}$  solution. The  $K_7\text{-Hg}^{2+}$  sensor was able to detect GSH with a detection limit of 0.3  $\mu\text{M}$ . This method was successfully

applied to GSH detection in FBS and human serum, yielding reproducible and reliable results. The influence of Hcy was not examined. However, since the stability constant of the  $K_7\text{-Hg}^{2+}$  complex was determined to be  $4 \times 10^6 \text{ M}^{-1}$  – significantly lower than those of the corresponding biothiol- $\text{Hg}^{2+}$  complexes – it was likely that the sensor could not discriminate among GSH, Cys, and Hcy.<sup>87</sup>

Among the complexes of  $\text{Hg}^{2+}$  ions, one complex was also reported to selectively detect Cys in the presence of other biothiols. The complex  $(K_8)_2\text{-Hg}^{2+}$ , formed between  $\text{Hg}^{2+}$  and a fluorescent compound  $K_8$  (a BODIPY derivative) in a 2 : 1 molar ratio, was described by Monu Kumar and co-authors. This complex exhibits the ability to selectively detect Cys in the presence of GSH, Hcy, and other amino acids *via* a reversible decomplexation mechanism, following an OFF/ON fluorescence mode (Fig. 36). The detection limit for Cys was estimated to be 0.029  $\mu\text{M}$  in DMF/ $\text{H}_2\text{O}$  (1 : 9, v/v, 10 mM HEPES buffer, pH 8.0). The reversibility and reusability of  $(K_8)_2\text{-Hg}^{2+}$  were demonstrated for up to five cycles by sequential addition of Cys and



$\text{Hg}^{2+}$ . The structure of  $(\text{K}_8)_2\text{-Hg}^{2+}$  was confirmed by  $^1\text{H}$  NMR,  $^{11}\text{B}$  NMR,  $^{19}\text{F}$  NMR, and HRMS spectra. The study further revealed that adding Cys to a solution of  $(\text{K}_8)_2\text{-Hg}^{2+}$  (10  $\mu\text{M}$ ) at a Cys concentration of 20  $\mu\text{M}$  (corresponding to a Cys/ $\text{Hg}^{2+}$  molar ratio of 2) restored the fluorescence intensity almost completely to the level of free  $\text{K}_8$  (20  $\mu\text{M}$ ). However, experimental HRMS spectra indicated that the product formed after adding excess Cys to the  $(\text{K}_8)_2\text{-Hg}^{2+}$  solution possessed the structure  $(\text{Cys})_4\text{Hg}^{2+}$ . This suggested that the reaction between Cys and the initial  $(\text{K}_8)_2\text{-Hg}^{2+}$  complex produced  $(\text{Cys})_2\text{Hg}^{2+}$  and released free  $\text{K}_8$ , while excess Cys subsequently formed the  $(\text{Cys})_4\text{Hg}^{2+}$  complex. The selective reactivity of  $(\text{K}_8)_2\text{-Hg}^{2+}$  toward Cys rather than GSH or Hcy was attributed to the differences in the acid dissociation constants ( $\text{pK}_a$  values) of Cys, Hcy, and GSH (8.0, 8.87, and 9.20, respectively).<sup>88</sup>

Xiaoquan Lu and co-authors reported a sensor based on the complex of 5,10, 15, 20-(4-sulphonatophenyl)porphyrin ( $\text{K}_9$ ) with  $\text{Hg}^{2+}$ , which was capable of detecting GSH in a PBS buffer solution (25 mM, pH = 7) (Fig. 37). GSH reacted with the  $\text{K}_9\text{-Hg}^{2+}$  complex and released free  $\text{K}_9$ , resulting in a fluorescence turn-on response. The detection limit for GSH using the  $\text{K}_9\text{-Hg}^{2+}$  complex was reported to be extremely low, approximately 16 fM (*i.e.*,  $16 \times 10^{-9}$   $\mu\text{M}$ ). Notably, the  $\text{K}_9\text{-Hg}^{2+}$  sensor was able to selectively detect GSH in the presence of a wide range of metal ions and biomolecules, including  $\text{Mg}^{2+}$ ,  $\text{Na}^+$ ,  $\text{Ni}^{2+}$ ,  $\text{Cd}^{2+}$ ,  $\text{Mn}^{2+}$ ,  $\text{Co}^{2+}$ ,  $\text{Pb}^{2+}$ ,  $\text{Cu}^{2+}$ ,  $\text{Fe}^{3+}$ ,  $\text{Zn}^{2+}$ ,  $\text{Ag}^+$ , Gly, Lys, Ala, Arg, AA, Phg, VB<sub>2</sub>, His, and remarkably, even Cys. Unfortunately, the study did not investigate the effect of Hcy, nor did it discuss the mechanism underlying the selective recognition of GSH over Cys. This method was successfully applied to detect GSH in diluted real samples. The results showed that the average recovery rates of GSH in red grapes, cherry tomatoes, and calf serum ranged from 93.4–110.0%, 96.0–104.5%, and 97.0–100.7%, respectively. These findings demonstrated that the proposed method was applicable for the detection of GSH in real sample matrices.<sup>89</sup>

**3.2.2 The reaction between  $\text{Hg}^{2+}$  ions and biothiols.** Unlike  $\text{Cu}^{2+}$ , the reactions between  $\text{Hg}^{2+}$  and biothiols occurred purely through complexation processes, without involving any redox reactions.

For GSH (denoted as  $\text{H}_3\text{L}$ ), the product of its reaction with  $\text{Hg}^{2+}$  depended on both the GSH :  $\text{Hg}^{2+}$  molar ratio and the solution pH. At a 2 : 1 GSH :  $\text{Hg}^{2+}$  ratio, with pH values ranging from 3 to 9, the predominant product was  $\text{HgL}_2\text{H}_2$  (charges not shown); at approximately pH 9.5, the main product was  $\text{HgL}_2\text{H}$ ; and between pH 9.5 and 12.0,  $\text{HgL}_2$  became the dominant species. At a 1 : 1 GSH :  $\text{Hg}^{2+}$  ratio, the dominant species were  $\text{HgLH}_2$  at pH 2.0–3.3,  $\text{HgLH}$  at pH 3.3–6.5,  $\text{HgL}$  at pH 6.5–10.3, and  $\text{HgL(OH)}$  above pH 10.3. At neutral pH, even when the GSH :  $\text{Hg}^{2+}$  molar ratio increased to 22 : 1, the  $\text{HgL}_2$  species still accounted for 95% of the total complexes formed. The logarithmic stability constants ( $\log \beta$ ) for  $\text{HgL}_2$  and its protonated forms ( $\text{HgL}_2\text{H}$ ,  $\text{HgL}_2\text{H}_2$ , and  $\text{HgL}_2\text{H}_3$ ) were 33.40, 42.40, 52.29, and 55.28, respectively. The  $\log \beta$  values for  $\text{HgL}$  and its related species ( $\text{HgLH}$ ,  $\text{HgLH}_2$ , and  $\text{HgL(OH)}$ ) were 26.04, 32.49, 35.68, and 15.80, respectively.<sup>90,91</sup>

For Cys (denoted as  $\text{H}_2\text{L}'$ ), although no detailed studies had been conducted on its reaction products with  $\text{Hg}^{2+}$  – unlike the well-documented case of GSH and  $\text{Hg}^{2+}$  – it was theoretically inferred, based on solution-phase equilibrium principles, that the resulting species also depended on both the Cys :  $\text{Hg}^{2+}$  molar ratio and the solution pH. Experimental and theoretical studies have shown that Cys could coordinate with  $\text{Hg}^{2+}$  to form several complexes, including  $\text{HgL}'$ ,  $\text{HgL}'_2$ ,  $\text{HgL}'_2\text{H}$ ,  $\text{HgL}'_2\text{H}_2$ , and  $\text{Hg(L'H)}_2$ . The  $\log \beta$  value for the  $\text{HgL}'$  complex was reported with considerable variation, being 14.21 (at 25 °C, in 0.1 M  $\text{KNO}_3$ , using the glass electrode potentiometric method, Gl.) and 37.8 (at 25 °C, using the mercury electrode potentiometric method, Hg el.). The  $\log \beta$  value for the  $\text{HgL}'_2$  complex was found to be very high and relatively consistent across different techniques: 43.57 (at 25 °C, in 0.1 M  $\text{KNO}_3$ , using the polarographic method, Pol.), 44.0 (at 25 °C, using the Hg el. method), and 41.80 (at 25 °C, in 0.1 M  $\text{KNO}_3$ , using the Gl. method). The  $\log \beta$  values for the remaining complexes –  $\text{HgL}'_2\text{H}$ ,  $\text{HgL}'_2\text{H}_2$ , and  $\text{Hg(L'H)}_2$  – were approximately 54.37, 61.79, and 39.4, respectively.<sup>92</sup>

For Hcy (denoted as  $\text{H}_2\text{L}''$ ), published reports on its complexes with  $\text{Hg}^{2+}$  remained scarce. One rare investigation determined the  $\log \beta$  value for the  $\text{HgL}''_2$  complex to be 39.4,

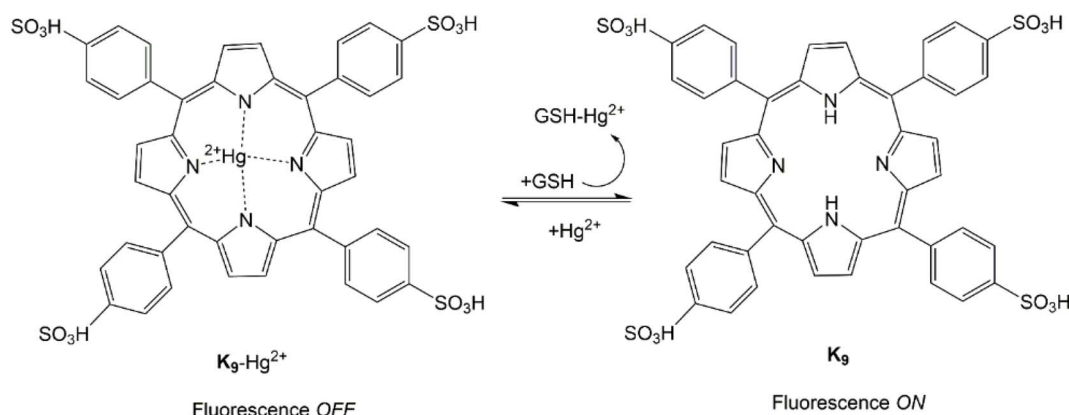


Fig. 37 The sensing mechanism of  $\text{K}_9\text{-Hg}^{2+}$  for GSH,<sup>89</sup> redrawn based on data reported in ref. 89, J. Chen, Q. Ma, X. Hu, Y. Gao, X. Yan, D. Qin and X. Lu, *Sens. Actuators B Chem.*, 2018, **254**, 475–482, copyright 2018.



suggesting that the complex formed between Hcy and  $\text{Hg}^{2+}$  was also highly stable.<sup>91</sup>

**3.2.3 Summary of fluorescent sensors for Biothiol detection based on  $\text{Hg}^{2+}$  complexes.** Although not as abundant as  $\text{Cu}^{2+}$  complexes,  $\text{Hg}^{2+}$  complexes still outnumbered other metal ions in applications as fluorescent sensors for biothiol detection. This might have been due to the fact that  $\text{Hg}^{2+}$  was not an essential element for life, which helped minimize background interference. Research results showed that sensors based on  $\text{Hg}^{2+}$  complexes could selectively detect biothiols in the presence of non-thiol amino acids, with detection limits ranging from  $16 \times 10^{-9}$  to  $0.47 \mu\text{M}$  (Table 4). The reaction mechanism involved only ligand exchange, forming  $\text{Hg}^{2+}$ -biothiol complexes and releasing the free ligand, without involving redox processes as observed in  $\text{Cu}^{2+}$  complexes. The reported stability constants of the sensing complexes ranged from  $5.8 \times 10^3$  to  $2.8 \times 10^{17}$  (Table 4), which were significantly lower than those of  $\text{Hg}^{2+}$ -biothiol complexes. Therefore, most sensors were unable to selectively detect individual thiols. An exception was  $(\text{K}_8)_2\text{-Hg}^{2+}$  (with a stability constant of  $2 \times 10^5$ ), which was reported to selectively detect Cys over GSH and Hcy at pH 8.0. The proposed reason for Cys selectivity was the difference in  $\text{pK}_a$  values of GSH, Cys, and Hcy (8.87, 8.0, and 9.20, respectively). However, this explanation was not entirely convincing, since at pH 8.0, the calculated conditional stability constants of  $\text{HgL}_2$ ,  $\text{HgL}_2$ , and  $\text{HgL}_2$  were  $10^{28.66}$ ,  $10^{34.80}$ , and  $10^{31.83}$ , respectively (here, the conditional stability constants,  $\beta'$ , were calculated according to the equation:  $\beta' = (\alpha^2) \times \beta$ , where  $\beta$  is the stability constant and  $\alpha$  is the mole fraction of  $[\text{L}^{2-}]$ ,  $[\text{L}'^{2-}]$ , and  $[\text{L}''^{2-}]$  at the corresponding pH values, as obtained from Tables 1–3), all of which were significantly higher than that of the  $(\text{K}_8)_2\text{-Hg}^{2+}$  complex. Similar to sensors based on  $\text{Cu}^{2+}$  complexes, a more reasonable explanation lay in steric factors affecting the accessibility and binding of thiols to the central metal ion. In addition, the  $\text{K}_9\text{-Hg}^{2+}$  complex was also reported to selectively detect GSH over Cys. Unfortunately, the stability constant of this complex was not reported, nor was the reason for its selectivity toward GSH over Cys discussed.

### 3.3 Sensors based the on complexation/decomplexation of other metal ions

**3.3.1 Sensors based on  $\text{Fe}^{3+}$  complexes.** Up to that point, numerous fluorescent sensors for  $\text{Fe}^{3+}$  detection, which operated through a reversible complexation mechanism with  $\text{Fe}^{3+}$  ions, had been reported. For example, more than 40 complexes had been investigated using rhodamine-based derivatives alone.<sup>93</sup> However, the number of  $\text{Fe}^{3+}$  complexes that had been examined for the detection of biothiols remained very limited. This might have been due to the fact that iron was an essential trace element for life in most organisms, including humans, animals, plants, and microorganisms. As a result, the influence of background iron (naturally present in samples) might have hindered the development of  $\text{Fe}^{3+}$  complexes for biothiol detection.

One of the very few fluorescent sensors that operated by this mechanism and was capable of detecting Cys in the presence of GSH and Hcy was reported by Ying Hu and co-authors in *Sensors and Actuators: B. Chemical* in 2023. In this work, an  $\text{L}_1\text{-Fe}^{3+}$  complex was formed between a pyrene-derived fluorophore ( $\text{L}_1$ ) and  $\text{Fe}^{3+}$  ions in a 1 : 1 molar ratio and was described as a selective fluorescent sensor for detecting Cys *via* an OFF–ON fluorescence mechanism (Fig. 38a). The reaction between  $\text{L}_1\text{-Fe}^{3+}$  and Cys occurred within approximately 50 seconds, over a wide pH range (from 2 to 11), and exhibited reversible cycling for at least 32 cycles (Fig. 38b). The detection limit for Cys was reported to be  $0.446 \mu\text{M}$ . Notably, this sensor selectively detected Cys in the presence of other thiols such as GSH and Hcy, as well as various non-thiol amino acids. The reason why  $\text{L}_1\text{-Fe}^{3+}$  reacted with Cys but not with GSH and Hcy was not clarified. Although the logarithmic stability constant of the  $\text{L}_1\text{-Fe}^{3+}$  complex had been determined to be 4.32, it was much lower than those of all  $\text{Fe}^{3+}$  complexes with Cys, GSH, and Hcy (as presented below). This sensor was successfully applied for the detection of Cys in various samples, including food samples, water samples, and human serum.<sup>94</sup>

**3.3.2 The reaction between  $\text{Fe}^{3+}$  ions and biothiols.** The reaction between  $\text{Fe}^{3+}$  and GSH ( $\text{H}_3\text{L}$ ) always involved a redox

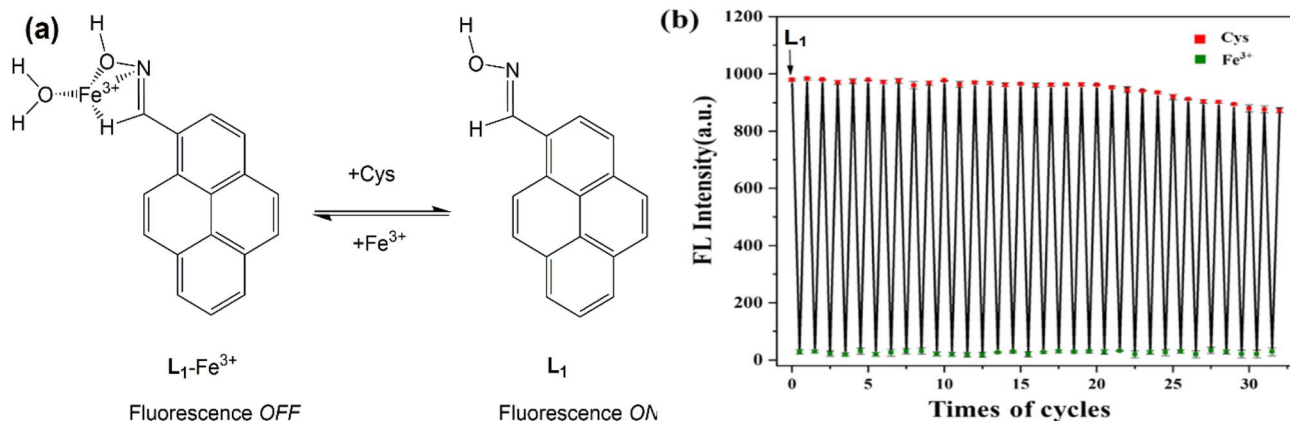


Fig. 38 (a) Fluorescent sensor for Cys based on the  $\text{L}_1\text{-Fe}^{3+}$  complex, (b) fluorescence changes of the sensor upon alternate addition of  $\text{Fe}^{3+}$  and  $\text{Hg}^{2+}$  ions,<sup>94</sup> adapted from ref. 94, Y. Hu, L. Lu, S. Guo, X. Wu, J. Zhang, C. Zhou, H. Fu and Y. She, *Sens. Actuators B Chem.*, 2023, **382**, 133534. Copyright 2023, with permission from Elsevier.



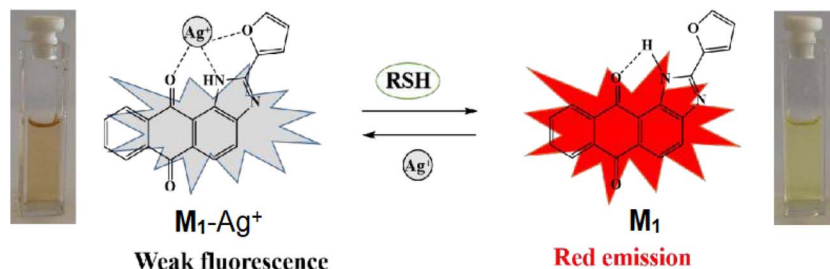


Fig. 39 Fluorescent sensor for biothiols based on the  $\text{Ag}^+$  complex of an anthraquinone–imidazole derivative ( $\text{M}_1\text{-Ag}^+$ ),<sup>106</sup> reproduced from ref. 106 with permission from the Royal Society of Chemistry, C. Zhao, X. Kong, S. Shuang, Y. Wang and C. Dong, *Analyst*, 2020, 145, 3029–3037, copyright 2020.

process. In the pH range from 3 to 7, the final products were  $\text{Fe}^{2+}$  complexes with either GSSG or GSH (when GSH was present in excess), in which the complexes were formed through bridging *via* carboxylate groups. At higher pH values, these complexes underwent hydrolysis to form  $\text{Fe}(\text{OH})_2$  precipitates. The complex between  $\text{Fe}^{2+}$  and GSSG existed mainly in two forms:  $\text{Fe-GSSG}$  and  $\text{Fe}_2\text{-GSSG}$ , where each  $\text{Fe}^{2+}$  ion formed two coordination bonds with two  $\text{-COO}^-$  groups in GSSG. The stability constants of these complexes were not reported. Meanwhile, the complex between  $\text{Fe}^{2+}$  and GSH was known to exist in the forms of  $\text{Fe}(\text{II})\text{LH}$ ,  $\text{Fe}(\text{II})(\text{LH})_2$ ,  $\text{Fe}(\text{II})\text{L}$ , and  $\text{Fe}(\text{II})\text{L}_2$ , with logarithmic stability constants of 9.81, 18.36, 17.5, and 32.06, respectively.<sup>95</sup>

$\text{Fe}^{3+}$  reacted with Cys ( $\text{H}_2\text{L}'$ ) to form the complexes  $\text{Fe}(\text{III})\text{L}'$ ,  $\text{Fe}(\text{III})\text{L}'_2$ , and  $\text{Fe}(\text{III})\text{L}'_3$ , with logarithmic stability constants of 10.85, 14.49, and 32.01, respectively. Similar to  $\text{Cu}^{2+}$ , the reaction between  $\text{Fe}^{3+}$  and Cys involved not only complex formation but also a redox process, which resulted in the formation of  $\text{Fe}^{2+}$  and cystine. The generated  $\text{Fe}^{2+}$  further reacted with Cys to form the complexes  $\text{Fe}(\text{II})\text{L}'$  and  $\text{Fe}(\text{III})\text{L}'_2$ , with logarithmic stability constants of 6.2 and 11.77, respectively.<sup>92,96</sup>

For Hcy, studies on the direct reactions between  $\text{Fe}^{3+}$  and  $\text{Fe}^{2+}$  with Hcy, as well as the stability constants of their complexes, had not been reported. However, based on the reactions and stability constants of  $\text{Fe}^{3+}$  and  $\text{Fe}^{2+}$  with Cys and GSH, it was evident that Hcy was also capable of forming very stable complexes with both  $\text{Fe}^{3+}$  and  $\text{Fe}^{2+}$ . In addition to complex formation, a redox reaction was also observed, in which  $\text{Fe}^{3+}$  was reduced to  $\text{Fe}^{2+}$  and Hcy was oxidized to HSSH (an oxidized form of Hcy). This redox reaction had also been described in studies on Hcy detection using electrochemical methods involving screen printed carbon electrode (SPE) and gold nanoparticle (GNP).<sup>97</sup>

**3.3.3 Sensors based on  $\text{Ag}^+$  complexes.** Up to that point, numerous complexes between  $\text{Ag}^+$  and fluorescent compounds had been reported; however, the number of complexes that had been employed as sensors for biothiol detection remained very limited.<sup>98–105</sup>

A rare example of a fluorescent sensor for biothiol detection based on a silver ion ( $\text{Ag}^+$ ) complex, formed *in situ* between the fluorophore  $\text{M}_1$  and  $\text{Ag}^+$  ions in a 1 : 1 molar ratio, was reported by Chen Zhao and co-workers (Fig. 39). The  $\text{M}_1\text{-Ag}^+$  complex was capable of detecting biothiols such as Cys, Hcy, and GSH

through a decomplexation process, with detection limits of 0.089, 0.174, and 0.208  $\mu\text{M}$ , respectively. In this study, the structure of the complex between  $\text{M}_1$  and  $\text{Ag}^+$  ions, as well as that between Cys and  $\text{Ag}^+$  ions, were confirmed using HRMS experimental spectra. The complex between Cys and  $\text{Ag}^+$  ions was identified to form in a 1 : 1 molar ratio, existing in the form of  $[\text{Ag} + \text{Cys-2H}]^-$ . The  $\text{M}_1\text{-Ag}^+$  sensor could be reused at least four times after detecting Cys by reintroducing  $\text{Ag}^+$  ions to reform the complex with the free  $\text{M}_1$  released from the decomplexation reaction. Furthermore, the  $\text{M}_1\text{-Ag}^+$  sensor was successfully employed to monitor biothiols in live.<sup>106</sup>

**3.3.4 The reaction between  $\text{Ag}^+$  and biothiols.** The results of solid-state and solution NMR analyses of the reaction products between  $\text{Ag}^+$  and biothiols indicated that all biothiols– $\text{Ag}^+$  complexes were coordinated through the S atom, might also have involved weak interactions through the O atom in the  $\text{-COO}^-$  group. Specifically, the complexes between  $\text{Ag}^+$  and Cys, Hcy, and GSH were proposed as illustrated in Fig. 40.<sup>107</sup>

Qiao Wu and colleagues conducted a detailed investigation of the reaction between  $\text{Ag}^+$  and GSH (designated as  $\text{H}_3\text{L}$ ) in solution, with the molar concentration ratio ( $K$ ) of biothiols to  $\text{Ag}^+$  ranging from 2.0 to 10.0 (at pH = 11). The results revealed that when  $K$  was small (2–3), a small amount of oligomeric species of the  $\text{GSH-Ag}^+$  complex tended to aggregate, in which, in addition to the strong S–Ag–S coordination bonds, weak  $\text{Ag}\cdots\text{Ag}$  interactions were also observed. When  $K$  increased, the  $\text{AgL}_2$  species became predominant in the solution.<sup>108</sup> Nevertheless, the stability constants of the complexes between  $\text{Ag}^+$  and GSH had not yet been reported.

Another study investigated in greater detail the reaction products between  $\text{Ag}^+$  and Cys (designated as  $\text{H}_2\text{L}'$ ). Under excess- $\text{Ag}^+$  conditions, the complex species identified were  $\text{AgHL}'$ ,  $\text{AgH}$ ,  $\text{Ag}_2\text{HL}'$ , and  $\text{Ag}_2\text{L}'$ , with corresponding logarithmic stability constants of 20.77, 11.14, 27.28, and 20.32. At pH values from 2 to about 5,  $\text{Ag}_2\text{HL}'$  was the predominant species, with  $\text{AgHL}'$  also present. Between pH 5 and 7,  $\text{AgHL}'$  became dominant, accompanied by  $\text{Ag}_2\text{HL}'$  and  $\text{Ag}_2\text{L}'$ . In the range of pH 7–9.8,  $\text{AgHL}'$  remained predominant, while  $\text{Ag}_2\text{HL}'$ ,  $\text{Ag}_2\text{L}'$ , and  $\text{AgL}'$  coexisted. From pH 9.8 to approximately 11,  $\text{AgL}'$  predominated, with  $\text{Ag}_2\text{L}'$  and  $\text{AgHL}'$  also present. All the complexes formed were proposed to be coordinated exclusively through Ag–S bonds.<sup>109</sup>



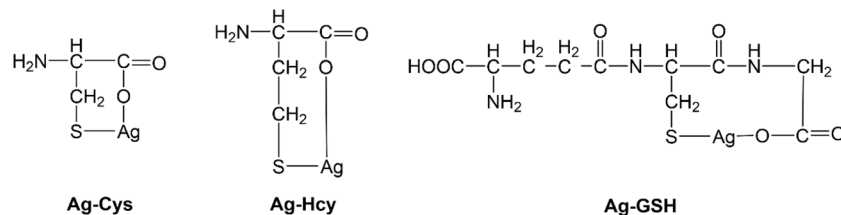


Fig. 40 The complexes between  $\text{Ag}^+$  and biothiols,<sup>107</sup> redrawn based on data reported in ref. 107.

To the best of our knowledge, no detailed studies had yet been published on the reaction between  $\text{Ag}^+$  and Hcy, nor on the stability constants of their complexes. However, based on previous research on Hcy detection using silver nanoparticles (AgNPs) and studies on the reactions between AgNPs and thiols, it was demonstrated that AgNPs, after being oxidized by dissolved oxygen in thiol-containing solutions, generated  $\text{Ag}^+$  ions, which subsequently interacted with thiols to form polymeric complex chains with various compositions and structures.<sup>110,111</sup> This behavior might have been one of the reasons why complexes between  $\text{Ag}^+$  and fluorescent compounds were rarely employed as sensors for thiol detection, in addition to other factors such as the aggregation of thiol- $\text{Ag}^+$  complexes when the  $\text{Ag}^+$  concentration exceeded that of thiols, or the intrinsic cytotoxicity of  $\text{Ag}^+$  ions to living cells.<sup>108,112–114</sup>

## 4 Summary and critical evaluation

In summary, fluorescent sensors based on metal complexation had exhibited outstanding characteristics in biothiol detection, including high selectivity and sensitivity, rapid response, operation under physiological conditions, applicability in living-cell studies, reversibility, and reusability. Among them, the complexes of  $\text{Cu}^{2+}$ ,  $\text{Hg}^{2+}$ ,  $\text{Fe}^{3+}$ , and  $\text{Ag}^+$  emerged as the most representative groups due to their strong coordination affinity toward thiol groups. Consequently, these sensors generally showed high selectivity and could detect biothiols in the presence of various amino acids, cations, and anions. Although most sensors were unable to distinguish among GSH, Hcy, and Cys, several metal complexes of  $\text{Cu}^{2+}$ ,  $\text{Hg}^{2+}$ ,  $\text{Fe}^{3+}$ , and  $\text{Ag}^+$  had been successfully developed to selectively detect individual biothiols. Moreover, each type of complex exhibited distinct advantages and disadvantages that should be carefully considered in further studies and applications.

The  $\text{Cu}^{2+}$  complexes were the most extensively employed, probably due to the high affinity of  $\text{Cu}^{2+}$  for biothiols, its relatively low toxicity to biological systems, and its minimal environmental and human health hazards. The major limitation, however, was the complexity of the reactions between  $\text{Cu}^{2+}$  and biothiols, which involved not only complex formation (with multiple possible coordination species) but also redox processes. As a result, the fluorescence signals often varied over time, limiting quantitative detection capabilities. Nevertheless, this redox behavior could also be exploited to design sensors with selective recognition for Hcy over GSH and Cys. Additionally, since  $\text{Cu}^{2+}$  is an essential metal ion in biological systems,

background interference could still occur during thiol analysis in biological matrices.

In contrast,  $\text{Hg}^{2+}$  complexes offered superior performance in terms of rapid response under mild conditions, since the extremely high stability constants of  $\text{Hg}^{2+}$ -thiol complexes ensured efficient ligand exchange and fluorescence recovery. Furthermore, their sensing mechanism was purely based on complexation without the interference of redox reactions. The minimal presence of mercury in biological systems reduced background interference. Moreover, at low concentrations,  $\text{Hg}^{2+}$  complexes exhibited limited cytotoxicity, making them promising for bioanalytical applications, particularly for real-time biothiol monitoring. However, the high toxicity of mercury and its potential environmental and health risks significantly restricted its practical applications. Therefore,  $\text{Hg}^{2+}$  complexes had been widely studied, second only to  $\text{Cu}^{2+}$  complexes.

Although a large number of  $\text{Fe}^{3+}$  complexes with fluorescent compounds had been reported, their application in biothiol detection was rarely investigated. This could have been attributed to the fact that iron is an essential element in biological systems, making it difficult to eliminate background interference. In addition, the reactions between  $\text{Fe}^{3+}$  and biothiols were rather complex, involving not only coordination but also redox and hydrolysis processes. Nevertheless, several  $\text{Fe}^{3+}$  complexes demonstrated remarkable properties, particularly the selective detection of Cys in the presence of GSH and Hcy, though the underlying mechanism had not yet been elucidated. Therefore, further exploration of  $\text{Fe}^{3+}$  complexes for biothiol detection remained worthwhile.

Regarding  $\text{Ag}^+$  complexes, although  $\text{Ag}^+$  exhibited strong affinity for biothiols, relatively few fluorescent sensors based on these complexes had been developed. This might have been due to the high cytotoxicity of  $\text{Ag}^+$  to biological systems. Moreover, the reactions between  $\text{Ag}^+$  and biothiols were also complicated. Although no redox process occurred, numerous complex species could form depending on the environment, and in some cases, aggregation or precipitation could take place, which posed significant challenges for experimental investigations.

## 5 Conclusion and future prospects

In summary, fluorescent sensors based on the complexation and decomplexation reactions of metal ions have proven to be highly effective tools for the detection of biothiols. Their excellent selectivity and sensitivity, reversible fluorescence response, and compatibility with physiological conditions make



these systems particularly attractive for biological and environmental analyses. Among them, complexes of  $\text{Cu}^{2+}$  and  $\text{Hg}^{2+}$  with fluorescent ligands have been the most extensively investigated, owing to the strong and stable coordination of these ions with biothiols and their oxidation products. Although  $\text{Fe}^{3+}$  and  $\text{Ag}^+$  are also capable of forming very stable complexes with biothiols, the high endogenous concentration of  $\text{Fe}^{3+}$  in living cells, which causes background interference, together with the cytotoxicity and precipitation issues associated with  $\text{Ag}^+$ , have limited their practical applications. In addition to complex formation,  $\text{Cu}^{2+}$ - and  $\text{Fe}^{3+}$ -based sensors also undergo redox reactions with biothiols.

Looking ahead, the future development of metal complex-based fluorescent sensors for biothiol detection should focus on several key directions:

(1) Continued development of fluorescent sensors based on metal ion complexes, prioritizing metal ions that demonstrate advantageous characteristics such as  $\text{Cu}^{2+}$  and  $\text{Hg}^{2+}$ . Efforts should be directed toward the use of highly emissive fluorophores to enhance sensor sensitivity, excitation and emission in the visible-light region to minimize photodamage during cellular studies, and small, water-soluble ligands to facilitate penetration through cellular membranes. Research should emphasize applications in biothiol detection within living cells for diagnostic and therapeutic purposes.

(2) Development of sensors capable of selectively detecting individual biothiols, guided by the insights and evaluations presented in this review. This could be achieved by considering factors such as steric effects, preferred redox mechanisms, or the conditional stability constants of metal complexes corresponding to the actual speciation of biothiols under various pH conditions.

(3) Further exploration of sensors that enable real-time monitoring of biothiols, based on the promising systems and mechanisms previously reported and discussed in this review.

(4) Integration of these sensors onto suitable materials to produce rapid testing devices, such as filter paper-based test strips for the detection of biothiols in human urine samples, as demonstrated in one of the studies discussed in this review.

(5) Combining theoretical calculations and simulations with experimental investigations to accelerate the understanding of sensing mechanisms and enable predictive control of fluorescence responses. In particular, theoretical studies could further clarify the structural and energetic factors governing metal-thiol coordination, thereby guiding the rational design of next-generation metal-based fluorescent sensors with enhanced stability, selectivity, and performance.

In conclusion, although remarkable progress has been achieved, there remains substantial room for innovation in the field of metal complex-based fluorescent sensors for biothiol detection. The continuous convergence of multiple disciplines in chemistry—particularly computational simulation, artificial intelligence, and experimental science—is expected to lead to the development of new sensing systems exhibiting high selectivity, high sensitivity, low toxicity, and real-time detection capability. Such advances will not only deepen the

understanding of fundamental chemical processes but also promote future biomedical and environmental applications.

## Conflicts of interest

There are no conflicts to declare.

## Data availability

No primary research results, software or code have been included and no new data were generated or analysed as part of this review.

Supplementary information (SI) is available. See DOI: <https://doi.org/10.1039/d5ra07368e>.

## Acknowledgements

This research was funded by the Vietnam National Foundation for Science and Technology Development (NAFOSTED) under grant number 104.06-2021.59 (Nguyen Khoa Hien).

## References

- G. Chwatko and E. Bald, *Talanta*, 2000, **52**, 509–515.
- C. X. Yin, K. M. Xiong, F. J. Huo, J. C. Salamanca and R. M. Strongin, *Angew. Chem., Int. Ed.*, 2017, **56**, 13188–13198.
- D. Chen and Y. Feng, *Crit. Rev. Anal. Chem.*, 2022, **52**, 649–666.
- S. M. Nabavi and A. S. Silva, *Nonvitamin and Nonmineral Nutritional Supplements*, Academic Press, 2018.
- Y. Yue, F. Huo, P. Ning, Y. Zhang, J. Chao, X. Meng and C. Yin, *J. Am. Chem. Soc.*, 2017, **139**, 3181–3185.
- D. Matuz-Mares, H. Riveros-Rosas, M. M. Vilchis-Landeros and H. Vázquez-Meza, *Antioxidants*, 2021, **10**, 1220.
- R. Vona, L. Pallotta, M. Cappelletti, C. Severi and P. Matarrese, *Antioxidants*, 2021, **10**, 201.
- J. Pizzorno, *Integr. Med. (Encinitas)*, 2014, **13**, 8–12.
- J. Selhub, *Annu. Rev. Nutr.*, 1999, **19**, 217–246.
- Y. Li, L. Chen, Y. Zhu, L. Chen, X. Yu, J. Li and D. Chen, *RSC Adv.*, 2021, **11**, 21116–21126.
- I. M. Graham, L. E. Daly, H. M. Refsum, K. Robinson, L. E. Brattström, P. M. Ueland, R. J. Palma-Reis, G. H. Boers, R. G. Sheahan and B. Israelsson, *JAMA*, 1997, **277**, 1775–1781.
- D. S. Wald, M. Law and J. K. Morris, *BMJ*, 2002, **325**, 1202.
- K. S. McCully, *Am. J. Pathol.*, 1969, **56**, 111.
- A. D. Smith, S. M. Smith, C. A. De Jager, P. Whitbread, C. Johnston, G. Agacinski, A. Oulhaj, K. M. Bradley, R. Jacoby and H. Refsum, *PLoS One*, 2010, **5**, e12244.
- M. Isokawa, T. Funatsu and M. Tsunoda, *Analyst*, 2013, **138**, 3802–3808.
- C.-J. Tsai, F.-Y. Liao, J.-R. Weng and C.-H. Feng, *J. Chromatogr. A*, 2017, **1524**, 29–36.
- I. M. Mostafa, H. Liu, S. Hanif, M. R. H. S. Gilani, Y. Guan and G. Xu, *Anal. Chem.*, 2022, **94**, 6853–6859.



- 18 P. Li, S. M. Lee, H. Y. Kim, S. Kim, S. Park, K. S. Park and H. G. Park, *Sci. Rep.*, 2021, **11**, 3937.
- 19 N. K. Hien, M. Van Bay, P. D. Tran, N. T. Khanh, N. D. Luyen, Q. V. Vo, D. U. Van, P. C. Nam and D. T. Quang, *RSC Adv.*, 2020, **10**, 36265–36274.
- 20 D. T. Nhan, N. K. Hien, H. Van Duc, N. T. A. Nhung, N. T. Trung, D. U. Van, W. S. Shin, J. S. Kim and D. T. Quang, *Dyes Pigm.*, 2016, **131**, 301–306.
- 21 H. J. Park, C. W. Song, S. Sarkar, Y. W. Jun, Y. J. Reo, M. Dai and K. H. Ahn, *Chem. Commun.*, 2020, **56**, 7025–7028.
- 22 L. Chen, Y. Feng, Y. Dang, C. Zhong and D. Chen, *Anal. Bioanal. Chem.*, 2020, **412**, 7819–7826.
- 23 D. Chen, Z. Long, Y. Sun, Z. Luo and X. Lou, *J. Photochem. Photobiol., A*, 2019, **368**, 90–96.
- 24 K. Dou, W. Huang, Y. Xiang, S. Li and Z. Liu, *Anal. Chem.*, 2020, **92**, 4177–4181.
- 25 G. Prabakaran and H. Xiong, *Food Chem.*, 2025, **464**, 141809.
- 26 L.-Y. Niu, Y.-Z. Chen, H.-R. Zheng, L.-Z. Wu, C.-H. Tung and Q.-Z. Yang, *Chem. Soc. Rev.*, 2015, **44**, 6143–6160.
- 27 O. Rusin, N. N. St. Luce, R. A. Agbaria, J. O. Escobedo, S. Jiang, I. M. Warner, F. B. Dawan, K. Lian and R. M. Strongin, *J. Am. Chem. Soc.*, 2004, **126**, 438–439.
- 28 W. Lin, L. Long, L. Yuan, Z. Cao, B. Chen and W. Tan, *Org. Lett.*, 2008, **10**, 5577–5580.
- 29 H. Wang, G. Zhou, H. Gai and X. Chen, *Chem. Commun.*, 2012, **48**, 8341–8343.
- 30 X. Yang, Y. Guo and R. M. Strongin, *Org. Biomol. Chem.*, 2012, **10**, 2739–2741.
- 31 E. C. Johnson and S. B. Kent, *J. Am. Chem. Soc.*, 2006, **128**, 6640–6646.
- 32 L.-Y. Niu, Y.-S. Guan, Y.-Z. Chen, L.-Z. Wu, C.-H. Tung and Q.-Z. Yang, *J. Am. Chem. Soc.*, 2012, **134**, 18928–18931.
- 33 L.-Y. Niu, Q.-Q. Yang, H.-R. Zheng, Y.-Z. Chen, L.-Z. Wu, C.-H. Tung and Q.-Z. Yang, *RSC Adv.*, 2015, **5**, 3959–3964.
- 34 J. Bouffard, Y. Kim, T. M. Swager, R. Weissleder and S. A. Hilderbrand, *Org. Lett.*, 2008, **10**, 37–40.
- 35 A. Shibata, K. Furukawa, H. Abe, S. Tsuneda and Y. Ito, *Bioorg. Med. Chem. Lett.*, 2008, **18**, 2246–2249.
- 36 M. H. Lee, Z. Yang, C. W. Lim, Y. H. Lee, S. Dongbang, C. Kang and J. S. Kim, *Chem. Rev.*, 2013, **113**, 5071–5109.
- 37 K. G. Reddie, W. H. Humphries, C. P. Bain, C. K. Payne, M. L. Kemp and N. Murthy, *Org. Lett.*, 2012, **14**, 680–683.
- 38 M. Mwafurirwa, K. Abdalla, W. Bian, H. Wei, L. Xu, W. Yu, Z. Hui, Q. Yang and X. Sun, *Smart Mol.*, 2024, **2**, e20240044.
- 39 Y. Hu, C. H. Heo, G. Kim, E. J. Jun, J. Yin, H. M. Kim and J. Yoon, *Anal. Chem.*, 2015, **87**, 3308–3313.
- 40 H. Jia, M. Yang, Q. Meng, G. He, Y. Wang, Z. Hu, R. Zhang and Z. Zhang, *Sensors*, 2016, **16**, 79.
- 41 W. Liu, J. Chen and Z. Xu, *Coord. Chem. Rev.*, 2021, **429**, 213638.
- 42 S. Maheshwari, Y. Li and M. J. Janik, *J. Electrochem. Soc.*, 2022, **169**, 064513.
- 43 M. Işık, D. Levorse, A. S. Rustenburg, I. E. Ndukwe, H. Wang, X. Wang, M. Reibarkh, G. E. Martin, A. A. Makarov and D. L. Mobley, *J. Comput.-Aided Mol. Des.*, 2018, **32**, 1117–1138.
- 44 A. V. Glushchenko and D. W. Jacobsen, *Antioxid. Redox Signaling*, 2007, **9**, 1883–1898.
- 45 M. Hepel and M. Stobiecka, *New Perspectives in Biosensors Technology and Applications*, 2011, pp. 343–372.
- 46 N. W. Pirie and K. G. Pinhey, *J. Biol. Chem.*, 1929, **84**, 321–333.
- 47 N. C. Li, O. Gawron and G. Bascuas, *J. Am. Chem. Soc.*, 1954, **76**, 225–229.
- 48 A. Mirzahassemi, M. Somlyay and B. Noszál, *Chem. Phys. Lett.*, 2015, **622**, 50–56.
- 49 A. Garcia, N. D. Eljack, M.-A. Sani, F. Separovic, H. H. Rasmussen, W. Kopec, H. Khandelia, F. Cornelius and R. J. Clarke, *Biochim. Biophys. Acta, Biomembr.*, 2015, **1848**, 2430–2436.
- 50 H. S. Jung, J. H. Han, T. Pradhan, S. Kim, S. W. Lee, J. L. Sessler, T. W. Kim, C. Kang and J. S. Kim, *Biomaterials*, 2012, **33**, 945–953.
- 51 D. C. Harris, *Quantitative Chemical Analysis*, Macmillan, 2010.
- 52 Q. Li, Y. Guo and S. Shao, *Sens. Actuators, B*, 2012, **171**, 872–877.
- 53 C.-C. Zhao, Y. Chen, H.-Y. Zhang, B.-J. Zhou, X.-J. Lv and W.-F. Fu, *J. Photochem. Photobiol., A*, 2014, **282**, 41–46.
- 54 S. Li, D. Cao, X. Meng, Z. Hu, Z. Li, C. Yuan, T. Zhou, X. Han and W. Ma, *Bioorg. Chem.*, 2020, **100**, 103923.
- 55 Y. Wang, H. Feng, H. Li, X. Yang, H. Jia, W. Kang, Q. Meng, Z. Zhang and R. Zhang, *Sensors*, 2020, **20**, 1331.
- 56 C. Li, X. Shang, Y. Chen, H. Chen and T. Wang, *J. Mol. Struct.*, 2019, **1179**, 623–629.
- 57 Y. Fu, H. Li, W. Hu and D. Zhu, *Chem. Commun.*, 2005, 3189–3191.
- 58 X.-F. Yang, P. Liu, L. Wang and M. Zhao, *J. Fluoresc.*, 2008, **18**, 453–459.
- 59 H. S. Jung, J. H. Han, Y. Habata, C. Kang and J. S. Kim, *Chem. Commun.*, 2011, **47**, 5142–5144.
- 60 P. Ruixue, L. Lili, W. Xiaoxia, L. Xiaohua and F. Xiaoming, *J. Org. Chem.*, 2013, **78**, 11602–11605.
- 61 S. Das, Y. Sarkar, R. Majumder, S. Mukherjee, J. Bandyopadhyay, A. Ray and P. P. Parui, *New J. Chem.*, 2017, **41**, 1488–1498.
- 62 Y. Wang, Q. Meng, Q. Han, G. He, Y. Hu, H. Feng, H. Jia, R. Zhang and Z. Zhang, *New J. Chem.*, 2018, **42**, 15839–15846.
- 63 O. G. Tsay, K. M. Lee and D. G. Churchill, *New J. Chem.*, 2012, **36**, 1949–1952.
- 64 M. Ahmed, *World Appl. Sci. J.*, 2014, **29**, 1357–1362.
- 65 K. Ngamchuea, C. Batchelor-McAuley and R. G. Compton, *Chem.-Eur. J.*, 2016, **22**, 15937–15944.
- 66 R. Österberg and R. Ligaarden, *J. Inorg. Biochem.*, 1979, **10**, 341–355.
- 67 N. Spear and S. D. Aust, *Arch. Biochem. Biophys.*, 1995, **324**, 111–116.
- 68 A. V. Kachur, C. J. Koch and J. E. Biaglow, *Free Radical Res.*, 1998, **28**, 259–269.
- 69 H. Speisky, M. Gómez, C. Carrasco-Pozo, E. Pastene, C. Lopez-Alarcón and C. Olea-Azar, *Bioorg. Med. Chem.*, 2008, **16**, 6568–6574.



- 70 H. Speisky, C. Lopez-Alarcon, C. Olea-Azar, C. Sandoval-Acuna and M. E. Aliaga, *Bioinorg. Chem. Appl.*, 2011, **2011**, 674149.
- 71 V. G. Shtyrlin, Y. I. Zyavkina, V. S. Ilakin, R. R. Garipov and A. V. Zakharov, *J. Inorg. Biochem.*, 2005, **99**, 1335–1346.
- 72 K. M. Dokken, J. G. Parsons, J. McClure and J. L. Gardea-Torresdey, *Inorg. Chim. Acta*, 2009, **362**, 395–401.
- 73 O. Yamauchi and A. Odani, *Pure Appl. Chem.*, 1996, **68**, 469–496.
- 74 M. D. Apostolova, P. R. Bontchev, B. B. Ivanova, W. R. Russell, D. R. Mehandjiev, J. H. Beattie and C. K. Nachev, *J. Inorg. Biochem.*, 2003, **95**, 321–333.
- 75 M. Gupta, J. Meehan-Atrash and R. M. Strongin, *Amino Acids*, 2021, **53**, 739–744.
- 76 M. Sibrian-Vazquez, J. O. Escobedo, S. Lim, G. K. Samoei and R. M. Strongin, *Proc. Natl. Acad. Sci.*, 2010, **107**, 551–554.
- 77 R. Zhao, J. Lind, G. Merenyi and T. E. Eriksen, *J. Am. Chem. Soc.*, 1994, **116**, 12010–12015.
- 78 W. Wang, J. O. Escobedo, C. M. Lawrence and R. M. Strongin, *J. Am. Chem. Soc.*, 2004, **126**, 3400–3401.
- 79 W. Wang, O. Rusin, X. Xu, K. K. Kim, J. O. Escobedo, S. O. Fakayode, K. A. Fletcher, M. Lowry, C. M. Schowalter and C. M. Lawrence, *J. Am. Chem. Soc.*, 2005, **127**, 15949–15958.
- 80 D. Wang, W. E. Crowe, R. M. Strongin and M. Sibrian-Vazquez, *Chem. Commun.*, 2009, 1876–1878.
- 81 P. Wardman, *J. Phys. Chem. Ref. Data*, 1989, **18**, 1637–1755.
- 82 N. Kaur, P. Kaur and K. Singh, *RSC Adv.*, 2014, **4**, 29340–29343.
- 83 A. K. Mahapatra, J. Roy, P. Sahoo, S. K. Mukhopadhyay, A. Banik and D. Mandal, *Tetrahedron Lett.*, 2013, **54**, 2946–2951.
- 84 G. Li, L. Ma, G. Liu, C. Fan and S. Pu, *RSC Adv.*, 2017, **7**, 20591–20596.
- 85 N. K. Hien, T. T. G. Chau, N. D. Luyen, Q. V. Vo, M. Van Bay, S. T. Ngo, P. C. Nam and D. T. Quang, *RSC Adv.*, 2025, **15**, 20125–20133.
- 86 Ş. N. Karuk Elmas, I. Berk Gunay, A. Karagoz, A. Bostanci, G. Sadi and I. Yilmaz, *Electroanalysis*, 2020, **32**, 775–780.
- 87 X. Wang, X. Ma, J. Wen, Z. Geng and Z. Wang, *Talanta*, 2020, **207**, 120311.
- 88 M. Kumar, G. Chaudhary and A. P. Singh, *Anal. Sci.*, 2021, **37**, 283–292.
- 89 J. Chen, Q. Ma, X. Hu, Y. Gao, X. Yan, D. Qin and X. Lu, *Sens. Actuators, B*, 2018, **254**, 475–482.
- 90 P. D. Oram, X. Fang, Q. Fernando, P. Letkeman and D. Letkeman, *Chem. Res. Toxicol.*, 1996, **9**, 709–712.
- 91 V. Liem-Nguyen, U. Skyllberg, K. Nam and E. Björn, *Environ. Chem.*, 2017, **14**, 243–253.
- 92 G. Berthon, *Pure Appl. Chem.*, 1995, **67**, 1117–1240.
- 93 S. K. Sahoo and G. Crisponi, *Molecules*, 2019, **24**, 3267.
- 94 Y. Hu, L. Lu, S. Guo, X. Wu, J. Zhang, C. Zhou, H. Fu and Y. She, *Sens. Actuators, B*, 2023, **382**, 133534.
- 95 M. Y. Hamed and J. Silver, *Inorg. Chim. Acta*, 1983, **80**, 115–122.
- 96 C. Canevali, A. Sansonetti, L. Rampazzi, D. Monticelli, M. D'Arienzo, B. Di Credico, E. Ghezzi, S. Mostoni, R. Nisticò and R. Scotti, *ChemPlusChem*, 2024, **89**, e202300709.
- 97 T. Madasamy, C. Santschi and O. J. Martin, *Analyst*, 2015, **140**, 6071–6078.
- 98 L. Xu, Y. Xu, W. Zhu, C. Yang, L. Han and X. Qian, *Dalton Trans.*, 2012, **41**, 7212–7217.
- 99 A. Affrose, S. D. S. Parveen, B. S. Kumar and K. Pitchumani, *Sens. Actuators, B*, 2015, **206**, 170–175.
- 100 K. Velmurugan, A. Raman, S. Easwaramoorthi and R. Nandhakumar, *RSC Adv.*, 2014, **4**, 35284–35289.
- 101 W.-T. Li, G.-Y. Wu, W.-J. Qu, Q. Li, J.-C. Lou, Q. Lin, H. Yao, Y.-M. Zhang and T.-B. Wei, *Sens. Actuators, B*, 2017, **239**, 671–678.
- 102 J. Sengottaiyan, K. Parvathi, S. Murukesan, B. Karpagam, J. Rajesh and G. Rajagopal, *ChemistrySelect*, 2025, **10**, e02804.
- 103 H.-X. Shi, W.-T. Li, Q. Li, H.-L. Zhang, Y.-M. Zhang, T.-B. Wei, Q. Lin and H. Yao, *RSC Adv.*, 2017, **7**, 53439–53444.
- 104 Y.-T. Wu, J.-L. Zhao, L. Mu, X. Zeng, G. Wei, C. Redshaw and Z. Jin, *Sens. Actuators, B*, 2017, **252**, 1089–1097.
- 105 G. Asaithambi and V. Periasamy, *Res. Chem. Intermed.*, 2019, **45**, 1295–1308.
- 106 C. Zhao, X. Kong, S. Shuang, Y. Wang and C. Dong, *Analyst*, 2020, **145**, 3029–3037.
- 107 A. A. Isab and M. I. Wazeer, *Spectrochim. Acta, Part A*, 2007, **66**, 364–370.
- 108 B. O. Leung, F. Jalilehvand, V. Mah, M. Parvez and Q. Wu, *Inorg. Chem.*, 2013, **52**, 4593–4602.
- 109 V. Alekseev, A. Semenov and P. Pakhomov, *Russ. J. Inorg. Chem.*, 2012, **57**, 1041–1044.
- 110 W. Leesutthiphonchai, W. Dungchai, W. Siangproh, N. Ngamrojnavanich and O. Chailapakul, *Talanta*, 2011, **85**, 870–876.
- 111 H. S. Toh, C. Batchelor-McAuley, K. Tschulik and R. G. Compton, *Sci. China: Chem.*, 2014, **57**, 1199–1210.
- 112 W. Fang, Z. Chi, W. Li, X. Zhang and Q. Zhang, *J. Nanobiotechnol.*, 2019, **17**, 66.
- 113 Z. Chi, H. Lin, W. Li, X. Zhang and Q. Zhang, *Environ. Sci. Pollut. Res.*, 2018, **25**, 32373–32380.
- 114 L. Yuan, T. Gao, H. He, F. Jiang and Y. Liu, *Toxicol. Res.*, 2017, **6**, 621–630.

